Quasi-local and frequency robust preconditioners for the Helmholtz first-kind integral equations on the disk

François Alouges, Martin Averseng

ESAIM: M2AN 58 (2024) 793–831
https://doi.org/10.1051/m2an/2023105

ESAIM: Mathematical Modelling and Numerical Analysis
www.esaim-m2an.org

QUASI-LOCAL AND FREQUENCY-ROBUST PRECONDITIONERS FOR THE HELMHOLTZ FIRST-KIND INTEGRAL EQUATIONS ON THE DISK

Francois Alouges[1] and Martin Averseng[2,*]

Abstract. We propose preconditioners for the Helmholtz scattering problems by a planar, disk-shaped screen in $\mathbb{R}^3$. Those preconditioners are approximations of the square-roots of some partial differential operators acting on the screen. Their matrix-vector products involve only a few sparse system resolutions and can thus be evaluated cheaply in the context of iterative methods. For the Laplace equation (*i.e.* for the wavenumber $k = 0$) with Dirichlet condition on the disk and on regular meshes, we prove that the preconditioned linear system has a bounded condition number uniformly in the mesh size. We further provide numerical evidence indicating that the preconditioners also perform well for large values of k and on locally refined meshes.

Mathematics Subject Classification. 65N38, 65F08, 35A21.

Received July 18, 2022. Accepted December 19, 2023.

1. Introduction

We consider the problem of acoustic scattering by a disk-shaped screen

$$\mathbb{D} := \left\{x = (x_1, x_2, 0) \in \mathbb{R}^3 \text{ such that } |x|^2 := x_1^2 + x_2^2 < 1\right\}$$

in $\mathbb{R}^3$, and its numerical simulation using the boundary element method (BEM). Calling $k \geq 0$ the wavenumber, with the convention that $k = 0$ for the Laplace equation, the problem can usually be rephrased as

$$V_k \lambda = f \quad \text{or} \quad W_k \mu = g \tag{1}$$

depending whether one considers a Dirichlet or Neumann boundary condition on the disk $\mathbb{D}$. Here λ and μ respectively stand for the jumps of the Neumann and Dirichlet traces of the scattered field across $\mathbb{D}$, while the weakly singular operator $V_k : \widetilde{H}^{-1/2}(\mathbb{D}) \to H^{1/2}(\mathbb{D})$ and the hypersingular operator $W_k : \widetilde{H}^{1/2}(\mathbb{D}) \to H^{-1/2}(\mathbb{D})$ are defined by

$$V_k\varphi := \int_{\mathbb{D}} G_k(x-y)\varphi(y)\,\mathrm{d}\sigma(y), \quad W_k\varphi := -\frac{\partial}{\partial n_x}\oint_{\mathbb{D}} \frac{\partial}{\partial n_y} G_k(x-y)\varphi(y)\,\mathrm{d}\sigma(y), \tag{2}$$

Keywords and phrases. Boundary element methods, preconditioning, singularities in PDEs.

[1] Département Mathématiques, Centre Borelli, ENS Paris-Saclay, 91190 Gif-sur-Yvette, France.
[2] Laboratoire Angevin de Recherche en Mathématiques, Université d'Angers, 2 Bd Lavoisier, 49000 Angers , France.
*Corresponding author: martin.averseng@univ-angers.fr

with $G_k(x) := \dfrac{e^{ik|x|}}{4\pi|x|}$ (the precise definitions are given in Sect. 3). Having computed λ or μ, the scattered field is finally explicitly obtained on $\mathbb{R}^3 \setminus \mathbb{D}$ through a classical representation formula (see *e.g.* [12,34]).

Solving the problem with the BEM involves the resolution of linear systems with the matrices $\mathbf{V}_k$ or $\mathbf{W}_k$ defined by

$$(\mathbf{V}_k)_{i,j} := \langle V_k \varphi_j, \varphi_i \rangle \quad \text{and} \quad (\mathbf{W}_k)_{i,j} := \langle W_k \psi_j, \psi_i \rangle,$$

where the boundary element basis $\{\varphi_i\}_{1\leq i\leq N_1} \subset \widetilde{H}^{-1/2}(\mathbb{D})$ and $\{\psi_i\}_{1\leq i\leq N_2} \subset \widetilde{H}^{1/2}(\mathbb{D})$ are sets of functions defined on a mesh of the screen $\mathbb{D}$, and the brackets stand for the duality products in $\widetilde{H}^{-1/2}(\mathbb{D}) \times H^{1/2}(\mathbb{D})$ and $H^{-1/2}(\mathbb{D}) \times \widetilde{H}^{1/2}(\mathbb{D})$ respectively. In the boundary element method, due to the non-local structure of the Green kernel G_k, the matrices $\mathbf{V}_k$ and $\mathbf{W}_k$ are fully populated, preventing *a priori* the use of fine meshes on the scatterer. However, in the past thirty years, several acceleration methods (*e.g.* the Fast Multipole Method [20,38], and H-Matrices [21]) have been developed that enable to compute the matrix-vector products $x \mapsto \mathbf{V}_k x, \mathbf{W}_k x$ in quasi-linear complexity. This allows to use iterative solvers for solving the underlying linear systems.

Nevertheless, when the problem of scattering by a bidimensional screen is considered, several difficulties still appear:

- The solutions of the integral equations have a well-known singularity at the edge of the screen (see *e.g.* [13]). In order to capture this singularity, the mesh needs to be refined locally near this edge [27].
- The condition number of the matrices $\mathbf{V}_k$ and $\mathbf{W}_k$ increases when the mesh is getting finer and this effect is aggravated by local mesh refinements, see *e.g.* [19].

Although preconditioning techniques for integral equations is a well established subject (see for instance [4, 5, 11, 41] and references therein), the extension of those ideas to singular domains has only be considered recently, *e.g.* by the authors in [3] (see also [10, 18, 24, 26]). The first goal of this work is to generalize the approach of [3] for 3D scattering problems on the disk $\mathbb{D}$ by introducing preconditioners that are robust both with respect to the mesh parameters and the wavenumber k.

By now, there is a well established strategy to ensure robustness with respect to the mesh parameters. For example, in the case of the operator V_k, it is sufficient to find an isomorphism $P : H^{1/2}(\mathbb{D}) \to \widetilde{H}^{-1/2}(\mathbb{D})$, together with a "stable discretisation" (see Sect. 4), to define a preconditioning matrix $\widehat{\mathbf{P}}$ associated to P. Then, it can be shown that the condition number of $\widehat{\mathbf{P}}\mathbf{V}_k$ is bounded by a constant that depends on k and P, but is otherwise independent of the mesh width. This property is often referred to as optimal preconditioning[1].

Nevertheless, an optimal preconditioner only guarantees a h-uniform bound on the condition number for a given, fixed k. There is no expected behavior when one considers different – and more specifically high – wave numbers. In practice, classical optimal preconditioners constructed for the Laplace equation ($k = 0$) behave poorly at high frequency (this is for example illustrated by our numerical results, cf. Tab. 15).

To counteract this negative behavior, the idea is thus to propose a family of operators $(P_k)_{k>0}$, that depend on the wavenumber k, such that the iterative resolution of the linear system associated to the matrix $\widehat{\mathbf{P}}_k\mathbf{V}_k$ involves a small number of iterations for a large range of values of k. Unfortunately, we are not aware of a general theory to estimate the number of iterations uniformly with respect to k (not even in the more favourable case of the scattering by a smooth surface without boundary), so for the time being, we must rely on numerical experiments to demonstrate the efficiency of the strategy (although we note that some k-explicit bounds on the number of iterations for second-kind integral equations have recently been shown, *e.g.* in [15]).

Let us now briefly outline the contents of this paper. Introducing the weight

$$\omega(x) := \sqrt{1 - x_1^2 - x_2^2}, \quad \text{for} \quad x \in \mathbb{D}, \tag{3}$$

[1]Note that strictly speaking a bound on the condition number does *not* directly imply a bound on the number of iterations in the iterative resolution of linear systems with non-normal matrices.

the main result of the paper is that

$$P_0 := \frac{1}{\omega}\left(-\omega \operatorname{div} \omega\nabla + \frac{1}{4}\mathrm{Id}\right)^{\frac{1}{2}}, \quad Q_0 := \omega(-\operatorname{div}\omega\nabla\omega)^{-\frac{1}{2}}$$

are spectrally equivalent to V_0^{-1}, and W_0^{-1}, respectively. Above and in what follows, Id stands for the identity operator, and $\omega \operatorname{div}\omega\nabla$ and $\operatorname{div}\omega\nabla\omega$ are understood as

$$(\omega \operatorname{div}\omega\nabla)\, u(x) = \omega(x)\operatorname{div}(\omega(x)\nabla u(x)), \quad (\operatorname{div}\omega\nabla\omega)\, u(x) = \operatorname{div}(\omega(x)\nabla(\omega(x)u(x))). \tag{4}$$

In other words, ω represents the multiplicative operator $(\omega u)(x) := \omega(x)u(x)$. The operators P_0 and Q_0 provide us with isomorphisms $H^{-1/2}(\mathbb{D}) \to \widetilde{H}^{-1/2}(\mathbb{D})$ and $H^{-1/2}(\mathbb{D}) \to \widetilde{H}^{1/2}(\mathbb{D})$ that, as we shall see, are cheaply evaluated when it comes to Galerkin discretization, and can be used efficiently as preconditioners for V_0 and W_0 respectively.

In order to proceed we introduce in Section 2 a scale of Hilbert spaces that conveniently replaces the classical Sobolev scale. This generalizes to the case of the disk in 3D, the scale introduced in [3] for open curves in 2D. Section 3 is then devoted to show the claimed result, *i.e.* the spectral equivalence of V_0^{-1} and P_0 on the one hand and W_0^{-1} and Q_0 on the other hand. For $k > 0$, our previous work [3] in dimension 2 suggests to generalize the preceding operators as:

$$P_k := \frac{1}{\omega}\left(-\omega \operatorname{div}\omega\nabla - k^2\omega^2\right)^{\frac{1}{2}}, \quad Q_k := \omega\left(-\operatorname{div}\omega\nabla\omega - k^2\omega^2\right)^{-\frac{1}{2}}.$$

The details on the Galerkin discretization, the efficient computation of the square roots, and the proofs of the uniform estimates of the condition number with respect to the mesh parameters are provided in Section 4. Eventually, the performance of the proposed preconditioners are reported in Section 5, and the implementation is openly available [7].

2. Weighted functional analysis on the disk

We now introduce some Hilbert scales $\mathcal{T}^s$ and $\mathcal{U}^s$ of functions on $\mathbb{D}$ that are weighted versions of Sobolev spaces especially well suited for the analysis of the considered problem. In those scales, the operators $-\omega \operatorname{div}\omega\nabla$ and $-\operatorname{div}\omega\nabla\omega$ are positive self-adjoint, allowing to define their square roots (as well as of some shifted versions), which are the main ingredient in our preconditiong strategy.

We start by introducing $L^2_{\frac{1}{\omega}}$ and L^2_ω the weighted L^2 spaces defined by

$$L^2_{\frac{1}{\omega}} := \left\{ u \in L^1_{loc}(\mathbb{D},\mathbb{C}) \;\middle|\; \|u\|^2_{\frac{1}{\omega}} := \int_{\mathbb{D}} \frac{|u(x)|^2}{\omega(x)}\,\mathrm{d}x < +\infty \right\},$$
$$L^2_\omega := \left\{ u \in L^1_{loc}(\mathbb{D},\mathbb{C}) \;\middle|\; \|u\|^2_{\omega} := \int_{\mathbb{D}} \omega(x)|u(x)|^2\,\mathrm{d}x < +\infty \right\},$$

with ω given by equation (3).

Those spaces, when equipped with the respective scalar products

$$\forall (u,v) \in \left(L^2_{\frac{1}{\omega}}\right)^2, \quad (u,v)_{\frac{1}{\omega}} := \int_{\mathbb{D}} \frac{u(x)\,\overline{v(x)}}{\omega(x)}\,\mathrm{d}x,$$
$$\forall (u,v) \in \left(L^2_{\omega}\right)^2, \quad (u,v)_{\omega} := \int_{\mathbb{D}} \omega(x)\,u(x)\,\overline{v(x)}\,\mathrm{d}x,$$

are Hilbert spaces.

Complete orthogonal families of these spaces are given by the following proposition (see [25,36]).

Proposition 2.1. *Let $\Lambda = \{(l,m) \in \mathbb{N} \times \mathbb{Z} \mid -l \leq m \leq l \text{ and } l-m \text{ is even}\}$, and let T_l^m and U_l^m be the functions defined for $(l,m) \in \Lambda$ and $x = (\rho, \varphi)$ by*

$$T_l^m(x) = Y_l^m(\arcsin(\rho), \varphi) \quad \text{and} \quad U_l^m(x) = \frac{Y_{l+1}^m(\arcsin(\rho), \varphi)}{\omega(x)}$$

where the function $Y_l^m(\theta,\varphi)$, $(\theta,\varphi) \in [0,\pi] \times [0,2\pi)$ are the classical spherical harmonics. The set $\{T_l^m\}_{(l,m)\in\Lambda}$ (resp. $\{U_l^m\}_{(l,m)\in\Lambda}$) is a complete orthogonal family of $L^2_{\frac{1}{\omega}}$ (resp. L^2_ω). The functions T_l^m and U_l^m satisfy in particular for all (l_1,m_1) and (l_2,m_2) in Λ,

$$\int_{\mathbb{D}} \frac{T_{l_1}^{m_1}(x)\,\overline{T_{l_2}^{m_2}(x)}}{\omega(x)}\,\mathrm{d}x = \frac{1}{2}\delta_{l_1=l_2}\delta_{m_1=m_2}, \quad \int_{\mathbb{D}} \omega(x)\,U_{l_1}^{m_1}(x)\,\overline{U_{l_2}^{m_2}(x)}\,\mathrm{d}x = \frac{1}{2}\delta_{l_1=l_2}\delta_{m_1=m_2}. \tag{5}$$

The functions T_l^m and U_l^m enjoy further properties. We provide the reader with a few of them that will turn out to prove useful in the following. Spherical harmonics are the restriction to the sphere of harmonic homogeneous polynomials in (x_1,x_2,x_3). Using this convention, one can write Y_l^m as

$$\begin{aligned} Y_l^m(x_1,x_2,x_3) &= \eta_l^m e^{im\phi} P_l^m(x_3) \\ &= \eta_l^m (x_1+ix_2)^m \frac{\mathrm{d}^{l+m}}{\mathrm{d}t^{l+m}}\left[\left(t^2-1\right)^l\right]_{|t=x_3}, \end{aligned}$$

where $\eta_l^m = (-1)^m\sqrt{\frac{(2l+1)}{4\pi}\frac{(l-m)!}{(l+m)!}}$ is a normalization coefficient that ensures $\int_{\mathbb{S}^2}|Y_l^m|^2\,\mathrm{d}\sigma = 1$, $(x_1,x_2) = (\rho\cos(\phi),\rho\sin(\phi))$ and P_l^m stand for the associated Legendre polynomials.

Using that, on the sphere, we have $x_3^2 = 1-x_1^2-x_2^2 = \omega(x)^2$, we can rewrite the spherical harmonics as polynomials for which the degree in the x_3 variables does not exceed 1. The T_l^m are obtained from the spherical harmonics that have a degree 0 in x_3, while the U_l^m are the ones obtained from the spherical harmonics of degree exactly 1 in x_3. Consequently, we deduce that the functions T_l^m and U_l^m are polynomial functions in (x_1,x_2), and a closer analysis shows that their degree is precisely l. We therefore deduce the following lemma, denoting by $C^\infty(\overline{\mathbb{D}})$ the set of restrictions to $\mathbb{D}$ of functions in $C^\infty(\mathbb{R}^2)$.

Lemma 2.2. *For all $(l,m) \in \Lambda$, the functions T_l^m and U_l^m are in $C^\infty(\overline{\mathbb{D}})$.*

A uniform bound can also be obtained by noticing that the spherical harmonics Y_l^m satisfy the addition formula

$$\sum_{m=-l}^{l} Y_l^m(\theta,\varphi)\overline{Y_l^m(\theta',\varphi')} = \frac{2l+1}{4\pi}P_l(a\cdot a')$$

where $P_l = P_l^0$ is the Legendre polynomial of degree l and a and a' are the points of the sphere with spherical coordinates (θ,φ) and (θ',φ') respectively. Applying this identity for $a = a' = (\rho\cos(\varphi),\rho\sin(\varphi),\sqrt{1-\rho^2})$, and since $P_l(1) = 1$, we conclude that for any $x = (\rho\cos(\varphi),\rho\sin(\varphi),0) \in \mathbb{D}$, and for any $l \in \mathbb{N}$,

$$\sum_{\substack{m=-l \\ m-l \text{ even}}}^{l} |T_l^m(x)|^2 \leq \sum_{m=-l}^{l} |Y_l^m(\arcsin\rho,\varphi)|^2 = \frac{2l+1}{4\pi}\cdot$$

In particular, this implies the bound, $\forall x \in \mathbb{D}$, $\forall (l,m) \in \Lambda$,

$$|T_l^m(x)| \leq \sqrt{\frac{2l+1}{4\pi}}\cdot \tag{6}$$

As a consequence of Proposition 2.1, any function $u \in L^2_{\frac{1}{\omega}}$ and $v \in L^2_{\omega}$ may be expanded in a Fourier-like series as

$$u(x) = \sum_{(l,m)\in\Lambda} \hat{u}_l^m T_l^m(x), \quad v(x) = \sum_{(l,m)\in\Lambda} \check{v}_l^m U_l^m(x),$$

where the series are converging in $L^2_{\frac{1}{\omega}}$ and L^2_{ω}, respectively, and

$$\forall (l,m) \in \Lambda, \quad \hat{u}_l^m = 2\int_{\mathbb{D}} \frac{u(x)\overline{T_l^m(x)}}{\omega(x)}\,\mathrm{d}x, \quad \check{v}_l^m = 2\int_{\mathbb{D}} \omega(x) v(x)\overline{U_l^m(x)}\,\mathrm{d}x.$$

The following Parseval equalities also hold:

$$\int_{\mathbb{D}} \frac{|u(x)|^2}{\omega(x)}\,\mathrm{d}x = \frac{1}{2}\sum_{(l,m)\in\Lambda} |\hat{u}_l^m|^2, \quad \int_{\mathbb{D}} \omega(x)|v(x)|^2\,\mathrm{d}x = \frac{1}{2}\sum_{(l,m)\in\Lambda} |\check{v}_l^m|^2. \tag{7}$$

We now use the following key lemma that enables us to define a scales of Hilbert spaces, comparable to the Sobolev spaces.

Lemma 2.3. *For all $(l,m) \in \mathbb{N}\times\mathbb{Z}$ such that $-l \le m \le l$, there holds*

$$-(\omega \operatorname{div} \omega\nabla)\, T_l^m = \big[l(l+1) - m^2\big] T_l^m, \tag{8}$$

$$-(\operatorname{div} \omega\nabla\omega)\, U_l^m = \big[(l+1)(l+2) - m^2\big] U_l^m. \tag{9}$$

We stress that the operators appearing on the left hand sides are understood as in equation (4).

Proof. We introduce the projected moments $\mathcal{L}_+$ and $\mathcal{L}_-$, defined for a regular enough function u defined on $\mathbb{D}$ by

$$\mathcal{L}_\pm u(\rho,\varphi) := e^{\pm i\varphi}\left(\pm\frac{\partial u}{\partial\rho} + i\frac{1}{\rho}\frac{\partial u}{\partial\varphi}\right).$$

Furthermore, we denote by $\omega\mathcal{L}_\pm\omega : C^\infty(\overline{\mathbb{D}}) \to C^\infty(\overline{\mathbb{D}})$ the operator defined by

$$(\omega\mathcal{L}_\pm\omega)\varphi(x) := \omega(x)\mathcal{L}_\pm(\omega(x)\varphi(x)) = \omega^2(x)\mathcal{L}_\pm\varphi(x) \mp \rho e^{\pm i\varphi}u(x).$$

Those operators are studied in [36], and their properties can be rephrased in our notation as follows: for all $(l,m) \in \Lambda$,

$$\mathcal{L}_\pm T_l^m = \sqrt{l(l+1) - m^2 \mp m}\; U_{l-1}^{m\pm1}, \tag{10}$$

$$\omega\mathcal{L}_\pm\omega U_l^m = \sqrt{(l+1)(l+2) - m^2 \mp m}\; T_{l+1}^{m\pm1}. \tag{11}$$

One easily checks that

$$\nabla = \frac{1}{2}\begin{pmatrix} \mathcal{L}_+ - \mathcal{L}_- \\ -i\mathcal{L}_+ - i\mathcal{L}_- \end{pmatrix}, \quad \omega\nabla\omega = \frac{1}{2}\begin{pmatrix} \omega\mathcal{L}_+\omega - \omega\mathcal{L}_-\omega \\ -i\omega\mathcal{L}_+\omega - i\omega\mathcal{L}_-\omega \end{pmatrix}, \tag{12}$$

which leads to the identities

$$\omega \operatorname{div} \omega\nabla = -\frac{(\omega\mathcal{L}_+\omega)\mathcal{L}_- + (\omega\mathcal{L}_-\omega)\mathcal{L}_+}{2},$$

$$\operatorname{div} \omega\nabla\omega = -\frac{\mathcal{L}_+(\omega\mathcal{L}_-\omega) + \mathcal{L}_+(\omega\mathcal{L}_-\omega)}{2},$$

and the result follows from equations (10) and (11). □

Definition 2.4 (Function spaces $\mathcal{T}^s$ and $\mathcal{U}^s$)**.** Let $\mathcal{T}$ and $\mathcal{U}$ be the complex vector spaces of formal series

$$\mathcal{T} = \left\{ \sum_{(l,m)\in\Lambda} \hat{u}_l^m T_l^m \;\middle|\; (\hat{u}_l^m)_{(l,m)\in\Lambda} \in \mathbb{C}^\Lambda \right\}, \quad \mathcal{U} = \left\{ \sum_{(l,m)\in\Lambda} \check{v}_l^m U_l^m \;\middle|\; (\check{v}_l^m)_{(l,m)\in\Lambda} \in \mathbb{C}^\Lambda \right\}.$$

For all $s \in \mathbb{R}$, we define the following Hilbert spaces:

$$\mathcal{T}^s := \{u \in \mathcal{T} \mid \|u\|_{\mathcal{T}^s} < \infty\}, \quad \mathcal{U}^s := \{v \in \mathcal{U} \mid \|v\|_{\mathcal{U}^s} < \infty\},$$

where

$$\|u\|_{\mathcal{T}^s}^2 := \frac{1}{2} \sum_{(l,m)\in\Lambda} |\hat{u}_l^m|^2 \left(\frac{1}{4} + l(l+1) - m^2\right)^s, \quad \|v\|_{\mathcal{U}^s}^2 := \frac{1}{2} \sum_{(l,m)\in\Lambda} |\check{v}_l^m|^2 \big((l+1)(l+2) - m^2\big)^s.$$

Note that, when $s \geq t$, $\mathcal{T}^s \subset \mathcal{T}^t$ and $\mathcal{U}^s \subset \mathcal{U}^t$. We adopt the notation

$$\mathcal{T}^{-\infty} := \cup_{s\in\mathbb{R}} \mathcal{T}^s, \quad \mathcal{T}^{\infty} := \cap_{s\in\mathbb{R}} \mathcal{T}^s, \quad \mathcal{U}^{-\infty} := \cup_{s\in\mathbb{R}} \mathcal{U}^s, \quad \mathcal{U}^{\infty} := \cap_{s\in\mathbb{R}} \mathcal{U}^s.$$

For $s \geq 0$, the convergent series in $\mathcal{T}^s$ and $\mathcal{U}^s$ are identified to their limits in $L^2_{\frac{1}{\omega}}(\mathbb{D})$ and $L^2_\omega(\mathbb{D})$ respectively, and in this case, one has

$$\hat{u}_l^m = \int_{\mathbb{D}} \frac{u(x)\,\overline{T_l^m(x)}}{\omega(x)}\,\mathrm{d}x, \quad \check{v}_l^m = \int_{\mathbb{D}} \omega(x) v(x)\,\overline{U_l^m(x)}\,\mathrm{d}x. \tag{13}$$

In this sense, $L^2_{\frac{1}{\omega}} \subset \mathcal{T}^s$ and $L^2_\omega \subset \mathcal{U}^s$ for all $s \leq 0$. Note that for $(u,v) \in L^2_{\frac{1}{\omega}} \times L^2_\omega$

$$\widehat{(\overline{u})}_l^m = (-1)^m \overline{\hat{u}_l^m}, \quad \widecheck{(\overline{u})}_l^m = (-1)^m \overline{\check{u}_l^m},$$

and this is taken as the definition of the complex conjugation on $\mathcal{T}^s$ and $\mathcal{U}^s$.

Notice the factor $\frac{1}{4}$ in the definition of the $\mathcal{T}^s$ norm and space that is conveniently taken for a reason that will appear clearer later (see Lem. 3.2). The following lemma shows that $C^\infty(\overline{\mathbb{D}})$ is a subset of $\mathcal{T}^s$ and $\mathcal{U}^s$ for all $s \in \mathbb{R}$:

Lemma 2.5. *Let $u \in C^\infty(\overline{\mathbb{D}})$ and $s \in \mathbb{R}$. Then $u \in \mathcal{U}^s$ and there exists $C_s > 0$ and $N_s \in \mathbb{N}$ such that*

$$\|u\|_{\mathcal{U}^s} \leq C_s \max_{|\alpha|\leq N_s} \|\partial^\alpha u\|_{L^\infty(\overline{\mathbb{D}})}$$

where $\alpha = (\alpha_1, \alpha_2) \in \mathbb{N}^2$ is a multi-index, $|\alpha| := \alpha_1 + \alpha_2$ and $\partial^\alpha u = \partial_{x_1}^{\alpha_1} \partial_{x_2}^{\alpha_2}$. The same statement holds replacing $\mathcal{U}^s$ by $\mathcal{T}^s$.

Proof. Let $u \in C^\infty(\overline{\mathbb{D}})$. We remark that $u \in L^2_\omega$ and therefore

$$\check{u}_l^m = 2 \int_{\mathbb{D}} \omega(x) u(x) \overline{U_l^m}(x)\,\mathrm{d}x$$

is well-defined. Now, noticing that

$$U_l^m(x) = \frac{-1}{((l+1)(l+2) - m^2)} \left[(\operatorname{div} \omega \nabla \omega)\, U_l^m\right](x)$$

and using the previous equality, an integration by parts gives

$$\check{u}_l^m = \frac{-2}{((l+1)(l+2)-m^2)} \int_{\mathbb{D}} \omega(x)[(\operatorname{div}\omega\nabla\omega)\, u](x)\overline{U_l^m(x)}\,\mathrm{d}x,$$

where we have used that ω vanishes on $\partial\mathbb{D}$ to suppress the boundary terms.

This argument can be repeated to obtain, for any $p \in \mathbb{N}$,

$$\check{u}_l^m = (-1)^p \frac{2}{((l+1)(l+2)-m^2)^p} \int_{\mathbb{D}} \omega(x)[(\operatorname{div}\omega\nabla\omega)^p u](x)\overline{U_l^m(x)}\,\mathrm{d}x.$$

We now remark that $\nabla\omega = \frac{x}{\omega}$, which entails that, for u regular enough,

$$(\operatorname{div}\omega\nabla\omega)u(x) = 2u(x) - x\cdot\nabla u(x) + \omega^2(x)\Delta u(x).$$

A simple reasoning by induction shows that $(\operatorname{div}\omega\nabla\omega)^p$ is a partial differential operator of the form

$$(\operatorname{div}\omega\nabla\omega)^p = \sum_{|\alpha|\le 2p} c_\alpha(x)\partial^\alpha,$$

where, for all multi-index α such that $|\alpha| \le 2p$, $c_\alpha \in C^\infty(\overline{\mathbb{D}})$. (In fact, the coefficients c_α are polynomials in x.) Thus for all p, there exists a constant $K_p > 0$ such that

$$|\check{u}_l^m| \le \frac{K_p \max_{|\alpha|\le 2p}\|\partial^\alpha u\|_{L^\infty(\mathbb{D})}}{((l+1)(l+2)-m^2)^p}.$$

For any $s \in \mathbb{R}$, we may take p sufficiently large to ensure that

$$K_s := \sum_{(l,m)\in\Lambda} ((l+1)(l+2)-m^2)^{s-2p} < +\infty.$$

We thus deduce that $u \in \mathcal{U}^s$ and

$$\|u\|_{\mathcal{U}^s} \le C_s \max_{|\alpha|\le 2p} \|\partial^\alpha u\|_{L^\infty(\overline{\mathbb{D}})}$$

where $C_s = \sqrt{K_s}K_p$. With the same method of proof, one can show the analogous result for $\mathcal{T}^s$. □

It is easy to check that the sequence of truncated series of an element of $\mathcal{T}^s$ or $\mathcal{U}^s$ converges to this element in the same space. Hence the set of finite linear combinations of $\{T_l^m\}_{(l,m)\in\Lambda}$ (resp. $\{U_l^m\}_{(l,m)\in\Lambda}$) is dense in $\mathcal{T}^s$ (resp. $\mathcal{U}^s$) for all $s \in \mathbb{R}$. It follows from this, Lemmas 2.5 and 2.2 that $C^\infty(\overline{\mathbb{D}})$ is also dense in $\mathcal{T}^s$ and $\mathcal{U}^s$ for all real s.

Lemma 2.6. *For all $s' < s$, the inclusions $\mathcal{T}^s \subset \mathcal{T}^{s'}$ and $\mathcal{U}^s \subset \mathcal{U}^{s'}$ are compact and dense.*

Proof. The fact that the inclusions are dense follows from the previous remark. Let us show the claim concerning the compact inclusion $\mathcal{T}^s \subset \mathcal{T}^{s'}$. The proof of the result for the spaces $\mathcal{U}^s$ goes along similar lines. Let $s \in \mathbb{R}$ and $s' = s - \delta$ for some $\delta > 0$. We have to show that $\mathcal{T}^s$ is compactly embedded in $\mathcal{T}^{s-\delta}$, or equivalently, that if $(u^n)_n$ is a sequence that weakly converges to 0 in $\mathcal{T}^s$, then $(u^n)_n$ strongly converges to 0 in $\mathcal{T}^{s-\delta}$. Writing

$$u^n = \sum_{(l,m)\in\Lambda} (\hat{u}_l^m)^n T_l^m,$$

the weak $\mathcal{T}^s$ convergence entails that both the following statements hold:

$$\exists C > 0,\ \forall n \in \mathbb{N},\quad \|u^n\|_{\mathcal{T}^s}^2 = \sum_{(l,m)\in\Lambda} \left(\frac{1}{4} + l(l+1) - m^2\right)^s |(\hat{u}_l^m)^n|^2 < C, \tag{14}$$

$$\forall (l,m)\in\Lambda,\qquad \lim_{n\to+\infty}(\hat{u}_l^m)^n=0. \tag{15}$$

Now, let $\varepsilon>0$ and $L(\varepsilon)\in\mathbb{N}$ be such that

$$\left(\frac{1}{4}+L(\varepsilon)\right)^{-\delta}\leq\varepsilon, \tag{16}$$

we infer, noticing that, for all $(l,m)\in\Lambda$, $\frac{1}{4}+l(l+1)-m^2\geq\frac{1}{4}+l$,

$$\begin{aligned}\|u^n\|_{\mathcal{T}^{s-\delta}}^2&=\sum_{(l,m)\in\Lambda}\left(\frac{1}{4}+l(l+1)-m^2\right)^{s-\delta}|(\hat{u}_l^m)^n|^2\\&=\sum_{(l,m)\in\Lambda,l\leq L(\varepsilon)}\left(\frac{1}{4}+l(l+1)-m^2\right)^{s-\delta}|(\hat{u}_l^m)^n|^2+\sum_{(l,m)\in\Lambda,l\geq L(\varepsilon)+1}\left(\frac{1}{4}+l(l+1)-m^2\right)^{s-\delta}|(\hat{u}_l^m)^n|^2\\&\leq\sum_{(l,m)\in\Lambda,l\leq L(\varepsilon)}\left(\frac{1}{4}+l(l+1)-m^2\right)^{s-\delta}|(\hat{u}_l^m)^n|^2+C\varepsilon\end{aligned}$$

using (14) and (16). By equation (15), we can now take n sufficiently large so that the first sum is smaller than ε, concluding the proof. □

Lemma 2.7. *For each $s\in\mathbb{R}$, the inner products $(\cdot,\cdot)_\omega$ and $(\cdot,\cdot)_{\frac{1}{\omega}}$ extend continuously to sesquilinear forms $\mathcal{U}^s\times\mathcal{U}^{-s}$ and $\mathcal{T}^s\times\mathcal{T}^{-s}$ respectively, and those extensions satisfy*

$$\forall(u,v)\in\mathcal{U}^s\times\mathcal{U}^{-s},\quad (u,v)_\omega=\frac{1}{2}\sum_{(l,m)\in\Lambda}\check{u}_l^m\overline{\check{v}_l^m}, \tag{17}$$

$$\forall(u,v)\in\mathcal{T}^s\times\mathcal{T}^{-s},\quad (u,v)_{\frac{1}{\omega}}=\frac{1}{2}\sum_{(l,m)\in\Lambda}\hat{u}_l^m\overline{\hat{v}_l^m}. \tag{18}$$

Proof. First, if u and v are finite linear combinations of the functions $(U_l^m)_{(l,m)\in\Lambda}$, then it follows immediately from equations (5) and (13) that

$$(u,v)_\omega=\frac{1}{2}\sum_{(l,m)\in\Lambda}\check{u}_l^m\overline{\check{v}_l^m}.$$

By density of such finite linear combinations in $\mathcal{U}^s$, it only remains to prove that the sesquilinear map

$$(u,v)\in\mathcal{U}^s\times\mathcal{U}^{-s}\mapsto\frac{1}{2}\sum_{(l,m)\in\Lambda}\check{u}_l^m\overline{\check{v}_l^m}$$

is continuous. This is indeed the case by the Cauchy–Schwarz inequality:

$$\left|\sum_{(l,m)\in\Lambda}\check{u}_l^m\overline{\check{v}_l^m}\right|^2\leq\sum_{(l,m)\in\Lambda}\left((l+1)(l+2)-m^2\right)^s|\check{u}_l^m|^2\sum_{(l,m)\in\Lambda}\left((l+1)(l+2)-m^2\right)^{-s}|\check{v}_l^m|^2=\|u\|_{\mathcal{U}^s}^2\|v\|_{\mathcal{U}^{-s}}^2.$$

The proof concerning the second inner product is similar. □

Lemma 2.8. *For every $s\in\mathbb{R}$, the maps $\frac{1}{\omega}:\mathcal{T}^{-s}\to(\mathcal{T}^s)'$ and $\omega:\mathcal{U}^{-s}\to(\mathcal{U}^s)'$, defined by*

$$\forall(u,v)\in\mathcal{T}^{-s}\times\mathcal{T}^s\quad\left(\frac{1}{\omega}u\right)(v):=(u,\overline{v})_{\frac{1}{\omega}},\quad\forall(u,v)\in\mathcal{U}^{-s}\times\mathcal{U}^s,\quad(\omega u)(v):=(u,\overline{v})_\omega,$$

are bijective isometries. With a slight abuse of notation, we also denote $\omega=\left(\frac{1}{\omega}\right)^{-1}:(\mathcal{T}^s)'\to\mathcal{T}^{-s}$.

The proof, mainly relying on the Riesz representation theorem, presents no difficulty, so we omit it.

Lemma 2.9. *For every $s \in \mathbb{R}$, the operators*

$$\nabla : C^\infty(\overline{\mathbb{D}}) \to \big(C^\infty(\overline{\mathbb{D}})\big)^2, \quad \operatorname{div} : \big(C^\infty(\overline{\mathbb{D}})\big)^2 \to C^\infty(\overline{\mathbb{D}}),$$

have unique extensions as linear continuous maps

$$\nabla : \mathcal{T}^s \to \big(\mathcal{U}^{s-1}\big)^2, \quad \operatorname{div} : (\mathcal{T}^s)^2 \to \mathcal{U}^{s-1}.$$

Proof. We perform the proof for the operator ∇, the other being similar. First, if such a linear continuous extension exists, it is unique by density of $C^\infty(\overline{\mathbb{D}})$ in $\mathcal{T}^s$ for all $s \in \mathbb{R}$. For $u \in C^\infty(\overline{\mathbb{D}})$ and $j \in \{1,2\}$, let $v = \partial_{x_j} u \in L^2_\omega$. Using integration by parts and the identities (11) and (12), we find

$$\begin{aligned}
\check{v}_l^m &= \big(\partial_{x_j} u, U_l^m\big)_\omega \\
&= -\big(u, (\omega \partial_{x_j} \omega) U_l^m\big)_{\frac{1}{\omega}} \\
&= \frac{1}{2} \begin{cases} -\sqrt{(l+1)(l+2) - m^2 - m}\big(u, T_{l+1}^{m+1}\big)_{\frac{1}{\omega}} + \sqrt{(l+1)(l+2) - m^2 + m}\big(u, T_{l+1}^{m-1}\big)_{\frac{1}{\omega}} & \text{if } j = 1, \\ i\sqrt{(l+1)(l+2) - m^2 - m}\big(u, T_{l+1}^{m+1}\big)_{\frac{1}{\omega}} + i\sqrt{(l+1)(l+2) - m^2 + m}\big(u, T_{l+1}^{m-1}\big)_{\frac{1}{\omega}} & \text{if } j = 2, \end{cases} \\
&= \frac{1}{4} \begin{cases} -\sqrt{(l+1)(l+2) - m^2 - m}\, \hat{u}_{l+1}^{m+1} + \sqrt{(l+1)(l+2) - m^2 + m}\, \hat{u}_{l+1}^{m-1} & \text{if } j = 1, \\ i\sqrt{(l+1)(l+2) - m^2 - m}\, \hat{u}_{l+1}^{m+1} + i\sqrt{(l+1)(l+2) - m^2 + m}\, \hat{u}_{l+1}^{m-1} & \text{if } j = 2. \end{cases}
\end{aligned}$$

Naturally, we use this expression as a definition for $\partial_{x_j} u$ when $u \in \mathcal{T}^{-\infty}$. Using simple estimates, such as $m \le (l+1)(l+2) - (m+1)^2$ when $(l,m) \in \Lambda$, we deduce that there exists a constant $C > 0$ such that

$$\begin{aligned}
\forall (l,m) \in \Lambda, \quad \big((l+1)(l+2) - m^2\big)^{\frac{s}{2}} \Big| \widetilde{(\partial_{x_j} u)}_l^m \Big| &\le C \left(\frac{1}{4} + (l+1)(l+2) - (m+1)^2 \right)^{\frac{s+1}{2}} \big|\hat{u}_{l+1}^{m+1}\big| \\
&\quad + C \left(\frac{1}{4} + (l+1)(l+2) - (m-1)^2 \right)^{\frac{s+1}{2}} \big|\hat{u}_{l+1}^{m-1}\big|.
\end{aligned}$$

This implies the desired continuity. □

Lemma 2.10. *For every $u \in T^1$, there holds*

$$\int_{\mathbb{D}} \omega(x) |\nabla u(x)|^2 \, \mathrm{d}x = \frac{1}{2} \sum_{(l,m) \in \Lambda} \big(l(l+1) - m^2\big) |\hat{u}_l^m|^2. \tag{19}$$

Proof. The two quadratic functionals

$$u \mapsto \int_{\mathbb{D}} \omega(x) |\nabla u(x)|^2 \, \mathrm{d}x, \quad u \mapsto \sum_{(l,m) \in \Lambda} \big(l(l+1) - m^2\big) |\hat{u}_l^m|^2$$

are continuous on $\mathcal{T}^1$. The continuity of the first functional is a special case of Lemma 2.9 with $s = 0$ (noting that $\mathcal{U}^0 = L^2_\omega$), while the second one stems from the definition of the $\mathcal{T}^1$ norm. Therefore, it suffices to show that

those functionals coincide on the dense subset of $\mathcal{T}^1$ consisting of the finite linear combinations of $\{T_l^m\}_{(l,m)\in\Lambda}$. If u is such a function, it is in particular twice differentiable, so we have by integration by parts

$$\int_{\mathbb{D}} \omega(x)|\nabla u(x)|^2\,\mathrm{d}x = \int_{\mathbb{D}} \frac{u(x)\overline{[-(\omega\,\mathrm{div}\,\omega\nabla)u](x)}}{\omega(x)}\,\mathrm{d}x = (u,v)_{\frac{1}{\omega}},$$

where $v = -(\omega\,\mathrm{div}\,\omega\nabla)u$. Using now Lemma 2.3, we have

$$v = \sum_{(l,m)\in\Lambda} (l(l+1)-m^2)T_l^m$$

and the result follows from the Parseval equality (18). □

The following weighted Poincaré inequality holds. To the best of our knowledge, this result is not of the kind that one may encounter in standard literature about weighted Poincaré inequalities, such as [28,35].

Theorem 2.11. *For all functions $u \in T^1$, there holds*

$$\int_{\mathbb{D}} \frac{|u(x)-u_\omega|^2}{\omega(x)}\,\mathrm{d}x \le \int_{\mathbb{D}} \omega(x)|\nabla u(x)|^2\,\mathrm{d}x, \tag{20}$$

where

$$u_\omega = \left(\int_{\mathbb{D}} \frac{1}{\omega(x)}\,\mathrm{d}x\right)^{-1} \int_{\mathbb{D}} \frac{u(x)}{\omega(x)}\,\mathrm{d}x.$$

Proof. It is easy to check that $u_\omega = \hat{u}_0^0 T_0^0$ since T_0^0 is constant on $\mathbb{D}$. We deduce the expression

$$\int_{\mathbb{D}} \frac{|u(x)-u_\omega|^2}{\omega(x)}\,\mathrm{d}x = \frac{1}{2}\sum_{(l,m)\in\Lambda, l\neq 0} |\hat{u}_l^m|^2.$$

For $(l,m)\in\Lambda$ with $l\neq 0$, we have $1 \le l(l+1)-m^2$ so

$$\int_{\mathbb{D}} \frac{|u(x)-u_\omega|^2}{\omega(x)}\,\mathrm{d}x \le \frac{1}{2}\sum_{(l,m)\in\Lambda} \big(l(l+1)-m^2\big)|\hat{u}_l^m|^2.$$

The right hand side is equal to $\int_{\mathbb{D}} \omega(x)|u(x)|^2\,\mathrm{d}x$ by Lemma 2.10, which proves the claim. □

Lemma 2.12. *Let*

$$X := -\omega\,\mathrm{div}\,\omega\nabla + \frac{1}{4}\mathrm{Id}, \quad Y := -\,\mathrm{div}\,\omega\nabla\omega. \tag{21}$$

Then X is a positive self-adjoint, unbounded operator on $L^2_{\frac{1}{\omega}}$, with domain $\mathcal{T}^2$. Similarly, Y is a positive self-adjoint, unbounded operator on L^2_ω with domain $\mathcal{U}^2$. They satisfy

$$X\left(\sum_{(l,m)\in\Lambda} \hat{u}_l^m T_l^m\right) = \sum_{(l,m)\in\Lambda} \left(\frac{1}{4}+l(l+1)-m^2\right)\hat{u}_l^m T_l^m,$$

$$Y\left(\sum_{(l,m)\in\Lambda} \check{u}_l^m U_l^m\right) = \sum_{(l,m)\in\Lambda} ((l+1)(l+2)-m^2)\check{u}_l^m U_l^m.$$

For all $\alpha, s\in\mathbb{R}$, the operators $X^\alpha : \mathcal{T}^s \to \mathcal{T}^{s-2\alpha}$ and $Y^\alpha : \mathcal{U}^s \to \mathcal{U}^{s-2\alpha}$ are continuous and

$$\|u\|_{\mathcal{T}^s}^2 = \frac{1}{2}\Big(X^{s/2}u, u\Big)_{\frac{1}{\omega}}, \quad \|u\|_{\mathcal{U}^s}^2 = \frac{1}{2}\Big(Y^{s/2}u, u\Big)_{\omega}.$$

Proof. For finite linear combinations of T_l^m or U_l^m, the formulas for X and Y are direct consequences of Lemma 2.3. The formulas in the general case follow by density. The proofs of the self-adjointness of X and Y follow standard arguments and we omit them for conciseness. The formulas for the $\mathcal{T}^s$ and $\mathcal{U}^s$ norms follow directly from the definitions. □

To conclude this section, we point out a characterization of the spaces $\mathcal{T}^\infty$ and $\mathcal{U}^\infty$. This plays no role in the remainder of the article, but the result is worth mentioning.

Theorem 2.13. *There holds* $\mathcal{T}^\infty = \mathcal{U}^\infty = C^\infty(\overline{\mathbb{D}})$.

The proof is given in Appendix A.

3. Parametrices for the integral operators

In this section, we define operators P_k and Q_k which will play the role of approximate inverses, or (weak) parametrices for the boundary integral operators V_k and W_k. They stand for the continuous versions of our proposed preconditioners, to be discretized in our numerical scheme. We start our discussion with the Laplace equation, *i.e.* $k = 0$.

3.1. Laplace layer potentials

We consider the following two sesquilinear forms $\mathcal{D}(\mathbb{D}) \times \mathcal{D}(\mathbb{D})$:

$$b_V(u,v) := \int_{\mathbb{D}}\int_{\mathbb{D}} \frac{u(x)\,\overline{v(y)}\,\mathrm{d}x\,\mathrm{d}y}{4\pi\|x-y\|},$$
$$b_W(u,v) := \int_{\mathbb{D}}\int_{\mathbb{D}} \frac{\mathbf{curl}\,u(x)\cdot\overline{\mathbf{curl}\,v(y)}\,\mathrm{d}x\,\mathrm{d}y}{4\pi\|x-y\|},$$

where $\mathbf{curl}\,u(x) := \begin{pmatrix}\partial_{x_2}u\\ -\partial_{x_1}u\end{pmatrix}$. They are well defined for smooth and compactly supported functions u and v on $\mathbb{D}$, and it is well-known that they extend uniquely to symmetric positive definite sesquilinear forms [42]

$$b_V : \widetilde{H}^{-1/2}(\mathbb{D}) \times \widetilde{H}^{-1/2}(\mathbb{D}) \to \mathbb{C}, \quad b_W : \widetilde{H}^{1/2}(\mathbb{D}) \times \widetilde{H}^{1/2}(\mathbb{D}) \to \mathbb{C}.$$

The spaces $H^s(\mathbb{D})$ and $\widetilde{H}^s(\mathbb{D})$ are the Sobolev spaces of complex distributions defined *e.g.* in Chapter 3 of [31]. The associated operators $V : \widetilde{H}^{-1/2}(\mathbb{D}) \to H^{1/2}(\mathbb{D})$ and $W : \widetilde{H}^{1/2}(\mathbb{D}) \to H^{-1/2}(\mathbb{D})$ such that

$$b_V(u,v) = \langle Vu, \overline{v}\rangle, \quad b_W(u,v) = \langle Wu, \overline{v}\rangle,$$

are known as the weakly singular and hypersingular integral operators. Here again, the notation $\langle\cdot,\cdot\rangle$ stand for both the duality pairings between $H^{-1/2}(\mathbb{D})$ and $\widetilde{H}^{1/2}(\mathbb{D})$ on the one hand, and between $\widetilde{H}^{-1/2}(\mathbb{D})$ and $H^{1/2}(\mathbb{D})$ on the other hand.

The fact that b_V and b_W are positive definite allows us to consider them as the inner products of $\widetilde{H}^{-1/2}(\mathbb{D})$ and $\widetilde{H}^{1/2}(\mathbb{D})$, respectively. Furthermore, we endow $H^{1/2}(\mathbb{D})$ and $H^{-1/2}(\mathbb{D})$ with the dual norms:

$$\|u\|_{H^{1/2}(\mathbb{D})} := \sup_{v\in\widetilde{H}^{-1/2}(\mathbb{D})} \frac{|\langle u,v\rangle|}{\|v\|_{\widetilde{H}^{-1/2}(\mathbb{D})}} \quad\text{and}\quad \|u\|_{H^{-1/2}(\mathbb{D})} := \sup_{v\in\widetilde{H}^{1/2}(\mathbb{D})} \frac{|\langle u,v\rangle|}{\|v\|_{\widetilde{H}^{1/2}(\mathbb{D})}}.$$

This is is equivalent to the norm defined *via* the Sobolev-Slobodeckij semi-norm, see Theorem 3.30 from [31].

The spaces $\mathcal{T}^s$ and $\mathcal{U}^s$ provide a good framework to analyze V and W. The main reason is the following result:

Proposition 3.1 (See [25,37]). *For any $(l,m)\in\Lambda$, one has*

$$V\left(\frac{T_l^m}{\omega}\right)=\frac{T_l^m}{2\lambda_l^m}\quad\text{and}\quad W(\omega U_l^m)=\frac{\lambda_{l+1}^m}{2}U_l^m$$

where

$$\lambda_l^m=2\frac{\Gamma\left(\frac{l+m+2}{2}\right)\Gamma\left(\frac{l-m+2}{2}\right)}{\Gamma\left(\frac{l+m+1}{2}\right)\Gamma\left(\frac{l-m+1}{2}\right)}$$

and $\Gamma(t)=\int_0^{+\infty}s^{t-1}e^{-s}\,\mathrm{d}s$ is the Gamma function.

The following estimate shows that $(\lambda_l^m)^2$ and the symbols of the weighted Laplacians (see Lem. 2.3), are equivalent:

Lemma 3.2. *One has the inequalities*

$$1\leq\frac{(\lambda_l^m)^2}{\frac14+l(l+1)-m^2}\leq\sqrt{3},\qquad l\in\mathbb{N},\ -l\leq m\leq l,\tag{22}$$

$$1\leq\frac{(\lambda_l^m)^2}{l(l+1)-m^2}\leq\sqrt{3},\qquad l\in\mathbb{N}^*,\ -l\leq m\leq l.\tag{23}$$

Proof. We start with the following improved version of Gautschi's inequality [29]:

$$\forall(x,s)\in\mathbb{R}_+^*\times(0,1),\quad\left(x+\frac{s}{2}\right)^{1-s}\leq\frac{\Gamma(x+1)}{\Gamma(x+s)}\leq\left(x-\frac12+\sqrt{s+\frac14}\right)^{1-s}.$$

We apply this inequality for $s=\frac12$, and notice that it remains true when $x=0$. We may therefore take $x=\frac{l\pm m}{2}$ to obtain

$$\left(l+m+\frac12\right)\left(l-m+\frac12\right)\leq(\lambda_l^m)^2\leq\left(l-m+\sqrt3-1\right)\left(l+m+\sqrt3-1\right).$$

Remarking that

$$\left(l+m+\frac12\right)\left(l-m+\frac12\right)=l(l+1)-m^2+\frac14$$

yields the left-hand side of the inequalities (22) and *a fortiori* (23).

For the right-hand side inequalities, we observe that for $l\geq2$ and $-l\leq m\leq l$, one has

$$\begin{aligned}\left(l+\sqrt3-1\right)^2-m^2&=l(l+1)-m^2+\left(2\sqrt3-3\right)l+4-2\sqrt3\\&\leq l(l+1)-m^2+\left(2\sqrt3-3\right)l+\left(4-2\sqrt3\right)\frac{l}{2}\\&\leq\sqrt3\left(l(l+1)-m^2\right)\end{aligned}$$

using that $l(l+1)-m^2\geq l$. This establishes the right hand side inequality of (23) for $l\geq2$, and one can check that the same inequality also holds for $l=1$. This also implies *a fortiori* the right hand side inequality of (22) for $l\neq0$, and again, one can check that it remains valid for $l=0$. □

Lemma 3.3. *There holds*

$$\widetilde{H}^{-1/2}(\mathbb{D})=\left(\mathcal{T}^{1/2}\right)',\quad\widetilde{H}^{1/2}(\mathbb{D})=\left(\mathcal{U}^{-1/2}\right)'\tag{24}$$

with the following norm equivalences:

$$\forall u\in\left(\mathcal{T}^{1/2}\right)',\quad 3^{-1/4}\|u\|_{\left(\mathcal{T}^{1/2}\right)'}\leq\sqrt2\|u\|_{\widetilde{H}^{-1/2}(\mathbb{D})}\leq\|u\|_{\left(\mathcal{T}^{1/2}\right)'},\tag{25}$$

$$\forall u\in\mathcal{U}^{1/2},\qquad 3^{-1/4}\|u\|_{\mathcal{U}^{1/2}}\leq\sqrt2\|\omega u\|_{\widetilde{H}^{1/2}(\mathbb{D})}\leq\|u\|_{\mathcal{U}^{1/2}}.\tag{26}$$

Proof. Consider $L \in \mathbb{N}$ and a function u of the form

$$u = \sum_{(l,m)\in\Lambda} \hat{u}_l^m T_l^m, \tag{27}$$

where $\hat{u}_l^m = 0$ for $l \geq L$. Putting $v = \frac{u}{\omega}$, we have, from Proposition 3.1:

$$Vv = \sum_{(l,m)\in\Lambda} \frac{\hat{u}_l^m}{2\lambda_l^m} T_l^m$$

hence $Vv \in C^\infty(\overline{\mathbb{D}})$. It follows that $v \in \widetilde{H}^{-1/2}(\mathbb{D})$ and

$$\|v\|^2_{\widetilde{H}^{-1/2}} = \int_{\mathbb{D}} (Vv)(x) \overline{\frac{u(x)}{\omega(x)}}\, \mathrm{d}x = \sum_{(l,m)\in\Lambda} \frac{|\hat{u}_l^m|^2}{2\lambda_l^m},$$

by the orthogonality properties of the T_l^m seen in the previous section. In view of the estimate (22), this implies

$$\frac{1}{2\sqrt{3}} \|u\|^2_{\mathcal{T}^{-1/2}} \leq \left\| \frac{1}{\omega} u \right\|^2_{\widetilde{H}^{-1/2}(\mathbb{D})} \leq \frac{1}{2} \|u\|^2_{\mathcal{T}^{-1/2}}. \tag{28}$$

Finally, by the density of finite linear combinations of the form (27) in $\mathcal{T}^{-1/2}$, it follows that $\frac{1}{\omega}\mathcal{T}^{-1/2} = \widetilde{H}^{-1/2}(\mathbb{D})$ with the norm equivalence (28) holding for all $u \in \mathcal{T}^{-1/2}$, where $\frac{1}{\omega}$ is understood as in Lemma 2.8. Since $\frac{1}{\omega}\mathcal{T}^{-1/2} = (\mathcal{T}^{1/2})'$, this proves the first norm equivalence (25). The proof of the second one is similar. □

Corollary 3.4. *There holds*

$$H^{1/2}(\mathbb{D}) = \mathcal{T}^{1/2}, \quad H^{-1/2}(\mathbb{D}) = \mathcal{U}^{1/2}$$

with the following norm equivalences:

$$\forall u \in \mathcal{T}^{1/2}, \quad \|u\|_{\mathcal{T}^{1/2}} \leq \frac{1}{\sqrt{2}} \|u\|_{H^{1/2}} \leq 3^{\frac{1}{4}} \|u\|_{\mathcal{T}^{1/2}}, \tag{29}$$

$$\forall u \in \mathcal{U}^{-1/2}, \quad \|u\|_{\mathcal{U}^{-1/2}} \leq \frac{1}{\sqrt{2}} \|u\|_{H^{-1/2}} \leq 3^{\frac{1}{4}} \|u\|_{\mathcal{U}^{-1/2}}. \tag{30}$$

We can now state the main result of this article. Recall the definitions of the operators X and Y in equation (21).

Theorem 3.5. *The operator $P = \frac{1}{\omega} X^{\frac{1}{2}}$ maps $H^{1/2}(\mathbb{D})$ to $\widetilde{H}^{-1/2}(\mathbb{D})$ bijectively and for all $u \in \widetilde{H}^{-1/2}(\mathbb{D})$, there holds*

$$\frac{1}{2} \|u\|^2_{H^{1/2}(\mathbb{D})} \leq \langle Pu, \overline{u} \rangle \leq \frac{\sqrt{3}}{2} \|u\|^2_{H^{1/2}(\mathbb{D})}.$$

The operator $Q = \omega Y^{-1/2}$ maps $H^{-1/2}(\mathbb{D})$ to $\widetilde{H}^{1/2}(\mathbb{D})$ bijectively and for all $u \in H^{-1/2}(\mathbb{D})$, there holds

$$\frac{1}{2} \|u\|^2_{H^{-1/2}(\mathbb{D})} \leq \langle Qu, \overline{u} \rangle \leq \frac{\sqrt{3}}{2} \|u\|^2_{H^{-1/2}(\mathbb{D})}.$$

Proof. By Lemma 2.12, we have, for all $u \in \mathcal{T}^{1/2}$, $\|u\|^2_{\mathcal{T}^{1/2}} = (\sqrt{X}u, u)_{\frac{1}{\omega}} = \langle Pu, \overline{u} \rangle$. The result follows by applying the second norm equivalence of Lemma 3.3. The proof for the second claim is similar. □

The previous result paves the way for a preconditioning strategy to solve the integral equation (1), that we present in Section 4.

3.2. Helmholtz layer potentials

We now seek corrections of the weighted Laplacians $-(\omega \operatorname{div} \omega\nabla)$ and $-(\operatorname{div} \omega\nabla\omega)$ in order to capture the behavior associated to non-zero wavenumbers. Let us first state a surprising commutation:

Theorem 3.6. *For any function $u \in C^\infty(\overline{\mathbb{D}})$, there holds*

$$\big(-\omega \operatorname{div} \omega\nabla - k^2\omega^2\big)V_{k,\omega}u = V_{k,\omega}\big(-\omega \operatorname{div} \omega\nabla - k^2\omega^2\big)u,$$

where $V_{k,\omega} = V_k \frac{1}{\omega}$ is the composition of the Helmholtz weakly-singular operator with the multiplication by $1/\omega$.

Proof. We observe that $\omega \operatorname{div} \omega\nabla$ is a self adjoint operator with respect to the scalar product $(\cdot,\cdot)_{\frac{1}{\omega}}$. Therefore, for any $u \in \mathcal{C}^\infty(\overline{\mathbb{D}})$, one has

$$\begin{aligned} V_{k,\omega}(\omega \operatorname{div} \omega\nabla u) &= \int_{\mathbb{D}} \frac{G_k(x-y)(\omega(y)\nabla_y \cdot (\omega(y)\nabla_y))u(y)}{\omega(y)} \,\mathrm{d}\sigma_y \\ &= \int_{\mathbb{D}} \frac{(\omega_y \operatorname{div}_y \omega_y\nabla_y G_k)(x-y)u(y)}{\omega(y)} \,\mathrm{d}\sigma_y. \end{aligned}$$

Let us denote

$$[V_{k,\omega}, \Delta_\omega] = V_{k,\omega}(\omega \operatorname{div} \omega\nabla)u - (\omega \operatorname{div} \omega\nabla)V_{k,\omega}u.$$

The previous computations then lead to

$$[V_{k,\omega}, \Delta_\omega]u = \int_{\mathbb{D}} \frac{\Delta(x,y)u(y)}{\omega(y)} \,\mathrm{d}\sigma_y$$

with

$$\Delta(x,y) = [\omega_y \operatorname{div}_y \omega_y\nabla_y - \omega_x \operatorname{div}_x \omega_x\nabla_x]G_k(x-y).$$

Using now the expression

$$\omega \operatorname{div} \omega\nabla\phi(x) = \omega^2(x)\Delta\phi(x) - x \cdot \nabla\phi(x)$$

we obtain

$$\Delta(x,y) = \Delta_x G_k(x-y)\big(\omega(y)^2 - \omega(x)^2\big) + (x+y) \cdot \nabla_x G_k(x-y). \tag{31}$$

We stress the fact that the Laplacian Δ_x used until now is the *bidimensional* Laplacian, which should not be mistaken with the *three dimensional* Laplacian of the Helmholtz equation, that we shall denote by $\Delta^{3\mathrm{D}}$. The Green function $G_k(x)$ satisfies the Helmholtz equation

$$\Delta_x^{3\mathrm{D}} G_k + k^2 G_k = \delta_0$$

where δ_0 is the Dirac mass at 0. Since G_k is a radial function, we may rewrite this latter equation, with a slight abuse of notation, as

$$G_k''(r) + \frac{2}{r}G_k'(r) + k^2 G_k(r) = \delta_0.$$

We deduce that

$$\begin{aligned} \nabla_x G_k(x) &= G_k'(r)\frac{x}{r} \\ &= -x\left(G_k''(r) + \frac{1}{r}G_k'(r) + k^2 G_k(r) - \delta_0\right) \\ &= -x\big(\Delta_x G_k(x) + k^2 G_k(x)\big) \end{aligned}$$

with $r = \|x\|$, using that $x\delta_0 = 0$. Plugging this expression in (31), we are led to

$$\Delta(x,y) = \Big(\omega^2(y) - \omega^2(x) + \|y\|^2 - \|x\|^2\Big)\Delta_x G_k(x-y) + k^2\Big(\|y\|^2 - \|x\|^2\Big)G_k(x-y).$$

Since $\omega(x) = \sqrt{1-\|x\|^2}$, the first term vanishes, and remarking that $\|y\|^2 - \|x\|^2 = \omega^2(x) - \omega^2(y)$, we may write

$$\begin{aligned}[V_{k,\omega}, \Delta_\omega]u &= k^2 \int_D \frac{\big(\omega^2(x) - \omega^2(y)\big)G_k(x-y)u(y)}{\omega(y)}\,\mathrm{d}\sigma_y \\ &= k^2\big(\omega^2 V_{k,\omega} - V_{k,\omega}\omega^2\big)u\end{aligned}$$

which proves the claim. □

To generalize our method for $k \neq 0$, we propose the operators

$$P_k = \frac{1}{\omega}\big(-\omega\,\mathrm{div}\,\omega\nabla - k^2\omega^2\big)^{\frac{1}{2}}, \quad Q_k = \omega\big(-\,\mathrm{div}\,\omega\nabla\omega - k^2\omega^2\big)^{-\frac{1}{2}}, \tag{32}$$

to play the role of parametrices for V_k and W_k, respectively. The insights that motivate this choice are the following:

- Taking $\omega \equiv 1$ and ignoring the singularity of the screen $\mathbb{D}$, the formula for P_k leads back to pseudo-differential approximations of the Dirichlet-to-Neumann (DtN) map which was successfully used for preconditioning purposes, see [4,5]. In the case of a flat screen, the DtN is simply a constant times the inverse of V_k, so the definition of P_k can be thought of as a generalization of this DtN approximation in the presence of an edge singularity.
- Using compact perturbation arguments, one can show that P_k and Q_k have the right mapping properties, *i.e.* $P_k : H^{1/2}(\mathbb{D}) \to \widetilde{H}^{-1/2}(\mathbb{D})$, and $Q_k : H^{-1/2} \to \widetilde{H}^{1/2}(\mathbb{D})$, are continuous, and continuously invertible for all but a countable set of values $k \in \mathbb{R}^+$.
- The above commutation implies that ωP_k and $V_{k,\omega}$ can be diagonalized in a common basis of eigenfunctions (one can check that the eigenfunctions of P_k turn out to be oblate spheroidal wave functions [14]). Hence, the product $V_k P_k = V_{k,\omega}(\omega P_k)$ is diagonal in this basis, while *a priori* $V_k P_0$ is not. This hints at the fact that $-k^2\omega^2$ is the "correct" k-dependent perturbation to add under the square-root. Perhaps, some fine eigenvalue estimates could show that $V_k P_k$ is close to a multiple of identity, although the required asymptotic results do not seem at reach for now.
- There is a striking analogy with the two-dimensional case [3], where a pseudo-differential analysis shows that, for the 2D analogs of P_k and Q_k, $-k^2\omega^2$ is the order zero perturbation of that leads to the most smoothing remainders R and R' in the formulas $V_k P_k = I_d/2 + R$, $W_k Q_k = I_d/2 + R'$, as measured in a suitable pseudo-differential scale [6].
- Eventually, the numerical evidence presented in Section 5 is very convincing.

Yet, a more rigorous justification of those choices remains to be proposed.

4. Galerkin discretization and preconditioners

4.1. Variational problems

Given some data $f \in H^{-1/2}(\mathbb{D})$ and $g \in H^{1/2}(\mathbb{D})$ and a wavenumber $k \geq 0$, we consider the following two variational formulations of the integral equation (1):

$$\text{Find } \lambda \in \widetilde{H}^{-1/2}(\mathbb{D}) \text{ such that } \forall \lambda' \in \widetilde{H}^{-1/2}(\mathbb{D}), \qquad \langle V_k\lambda, \lambda'\rangle = \langle f, \lambda'\rangle, \tag{33}$$

$$\text{Find } \mu \in \widetilde{H}^{1/2}(\mathbb{D}) \text{ such that } \forall \mu' \in \widetilde{H}^{1/2}(\mathbb{D}), \qquad \langle W_k\mu, \mu'\rangle = \langle g, \mu'\rangle. \tag{34}$$

We introduce two sequences of subspaces $\mathcal{V}_N \subset \widetilde{H}^{-1/2}(\mathbb{D})$ and $\mathcal{W}_M \subset \widetilde{H}^{1/2}(\mathbb{D})$ for $N, M \in \mathbb{N}$, and define the approximate solutions $(\lambda_N)_{N\in\mathbb{N}}$ and $(\mu_M)_{M\in\mathbb{N}}$ to the variational problems (33) and (34) by the Galerkin method as

$$\lambda_N \in \mathcal{V}_N, \quad \forall \lambda' \in \mathcal{V}_N, \quad \langle V_k \lambda_N, \lambda' \rangle = \langle f, \lambda' \rangle, \tag{35}$$
$$\mu_M \in \mathcal{W}_M, \quad \forall \mu' \in \mathcal{W}_M, \quad \langle W_k \mu_M, \mu' \rangle = \langle g, \mu' \rangle. \tag{36}$$

We introduce two basis $\{\varphi_i^N\}_{1\le i\le \dim \mathcal{V}_N}$ and $\{\psi_i^M\}_{1\le i\le \dim \mathcal{W}_M}$ of $\mathcal{V}_N$ and $\mathcal{W}_M$. The vectors Λ_N and U_M of coefficients of λ_N and μ_M in those respective basis are obtained by solving the systems

$$\mathbf{V}_k \Lambda_N = F_N, \tag{37}$$
$$\mathbf{W}_k U_M = G_M, \tag{38}$$

where $\mathbf{V}_k$ and $\mathbf{W}_k$ are the Galerkin matrices defined by

$$(\mathbf{V}_k)_{ij} = \langle V_k \varphi_i^N, \overline{\varphi_j}^N \rangle, \qquad 1 \le i, j \le \dim \mathcal{V}_N, \tag{39}$$
$$(\mathbf{W}_k)_{ij} = \left\langle W_k \psi_i^M, \overline{\psi_j}^M \right\rangle, \quad 1 \le i, j \le \dim \mathcal{W}_M, \tag{40}$$

with the column vectors

$$(F_N)_i = \left\langle f, \overline{\varphi_i^N} \right\rangle, \ 1 \le i \le \dim \mathcal{V}_N, \quad (G_M)_i = \left\langle g, \overline{\psi_i^M} \right\rangle, \ 1 \le i \le \dim \mathcal{W}_M. \tag{41}$$

The purpose of this section is to specify the choices of spaces $\mathcal{V}_N$ and $\mathcal{W}_M$ and their basis, and to define preconditioners $\widehat{\mathbf{P}}_k$ and $\widehat{\mathbf{Q}}_k$ for the dense linear systems (37) and (38) respectively. Furthermore, we estimate the condition number of the preconditioned linear system $\widehat{\mathbf{P}}_k \mathbf{V}_k$ in the special case of quasi-uniform meshes and $k = 0$.

In the remainder of this paper, the subscript k is omitted when $k = 0$, *i.e.* we write V, W, $\widehat{\mathbf{P}}$, $\widehat{\mathbf{Q}}$ instead of V_0, W_0, $\widehat{\mathbf{P}}_0$, $\widehat{\mathbf{Q}}_0$ and so on.

4.2. Abstract condition number estimate

In this paragraph, we fix $N \in \mathbb{N}$ and consider a subspace $\mathcal{X}_N \subset H^{1/2}(\mathbb{D})$ with $\dim \mathcal{X}_N = \dim \mathcal{V}_N$. Let $p : \mathcal{X}_N \times \mathcal{X}_N \to \mathbb{C}$ be a sesquilinear form that is continuous and coercive in the $\mathcal{T}^{1/2}$ norm on $\mathcal{X}_N$, *i.e.* such that

$$\exists c_p(N), C_p(N) > 0, \ \forall \theta \in \mathcal{X}_N, \quad c_p(N) \|\theta\|^2_{\mathcal{T}^{1/2}} \le p(\theta, \theta) \le C_p(N) \|\theta\|^2_{\mathcal{T}^{1/2}}. \tag{42}$$

We introduce a basis $\{\theta_i^N\}_{1\le i\le \dim \mathcal{X}_N}$ of $\mathcal{X}_N$ and define the square $N \times N$ matrices

$$\mathbf{P} := \left(p(\theta_i^N, \theta_j^N)\right)_{1\le i,j\le N}, \quad \mathbf{D} := \left(\left\langle \varphi_i^N, \overline{\theta_j^N} \right\rangle\right)_{1\le i,j\le N}. \tag{43}$$

With those definitions, let

$$\widehat{\mathbf{P}} := \mathbf{D}^{-1} \mathbf{P} \mathbf{D}^{-T}. \tag{44}$$

To analyze the preconditioning matrix $\widehat{\mathbf{P}}$, the key quantity, besides the constants $c_p(N)$ and $C_p(N)$ appearing in (42) is the following inf-sup stability constant (where the arguments in the infimum and supremum are always required to be non-zero)

$$\sigma(\mathcal{V}_N, \mathcal{X}_N) := \inf_{\varphi\in\mathcal{V}_N} \sup_{\theta\in\mathcal{X}_N} \frac{|\langle \varphi, \overline{\theta} \rangle|}{\|\varphi\|_{\widetilde{H}^{-1/2}} \|\theta\|_{H^{1/2}}}. \tag{45}$$

Indeed, we have the following result:

Theorem 4.1. *There holds*

$$\kappa\Big(\widehat{\mathbf{P}}\mathbf{V}\Big) \leq \frac{\sqrt{3}}{\sigma(\mathcal{V}_N,\mathcal{X}_N)^2}\frac{C_p(N)}{c_p(N)}$$

where $\kappa(\mathbf{M})$ *is the condition number of the matrix* $\mathbf{M}$*, defined as the ratio of the largest to the smallest singular value of* $\mathbf{M}$*.*

Proof. By Theorem 2.1 from [23], we have

$$\kappa(\hat{\mathbf{P}}\mathbf{V}) \leq \frac{\|a\|\|p\|\|d\|^2}{c_A c_P c_D^2} \tag{46}$$

where $a : \mathcal{V}_N \times \mathcal{V}_N \to \mathbb{C}$ and $d : \mathcal{V}_N \times \mathcal{W}_N \to \mathbb{C}$ are the sesquilinear forms defined by

$$\forall \varphi \in \mathcal{V}_N, \quad a(\varphi,\varphi) = \|\varphi\|^2_{\widetilde{H}^{-1/2}}, \quad d(\varphi,\theta) := \langle \varphi, \overline{\theta}\rangle,$$

and the constants appearing in the estimate are chosen so that

$$\begin{aligned}
c_A\|u\|^2_{\widetilde{H}^{-1/2}} \leq a(u,u) &\leq \|a\|\|u\|^2_{\widetilde{H}^{-1/2}},\\
|d(u,v)| &\leq \|d\|\|u\|_{\widetilde{H}^{-1/2}}\|v\|_{\mathcal{T}^{1/2}},\\
c_P\|u\|^2_{\mathcal{T}^{1/2}} \leq p(u,u) &\leq \|p\|\|u\|^2_{\mathcal{T}^{1/2}},\\
\inf_{\varphi_N\in\mathcal{V}_N}\sup_{\theta\in\mathcal{X}_N}\frac{|d(\varphi_N,\theta)|}{\|\theta\|_{\mathcal{T}^{1/2}}\|\varphi_N\|_{\widetilde{H}^{-1/2}}} &\geq c_D.
\end{aligned}$$

Since $a(u,u) = \|u\|^2_{\widetilde{H}^{-1/2}}$, we can take $c_A = \|a\| = 1$. Similarly, in view of (42), we can use $c_P = c_p(N)$ and we have $\|p\| \leq C_p(N)$. By the norm equivalence stated in Corollary 3.4,

$$|d(\varphi,\theta)| \leq \|\varphi\|_{\widetilde{H}^{-1/2}}\|\theta\|_{H^{1/2}} \leq 3^{1/4}\sqrt{2}\|\varphi\|_{\widetilde{H}^{-1/2}}\|\theta\|_{\mathcal{T}^{1/2}},$$

hence $\|d\| \leq 3^{1/4}\sqrt{2}$. Furthermore, combining the same norm equivalence with equation (45), we get

$$\forall \varphi_N \in \mathcal{V}_N, \quad \sup_{\theta\in\mathcal{X}_N}\frac{|d(\varphi_N,\theta)|}{\|\theta\|_{\mathcal{T}^{1/2}}} \geq \frac{\sqrt{2}}{3^{1/4}}\sigma(\mathcal{V}_N,\mathcal{X}_N)\|\varphi_N\|_{\widetilde{H}^{-1/2}}.$$

Hence we may take $c_D = \frac{\sqrt{2}}{3^{1/4}}\sigma(\mathcal{V}_N,\mathcal{W}_N)$. It remains to inject those values in the estimate (46) to conclude the proof. □

To apply this result concretely, we are going to

(i) specify spaces $\mathcal{V}_N$, $\mathcal{X}_N$ and estimate the constant $\sigma(\mathcal{V}_N,\mathcal{X}_N)$ of equation (45),
(ii) propose an explicit sesquilinear form p which satisfies (42), and estimate the ratio $C_p(N)/c_p(N)$.

4.3. Stable discretization with uniform meshes

We describe a stable discretization involving spaces of continuous piecewise linear functions, both for the operator and the preconditioner, over a sequence of globally quasi-uniform and shape-regular triangular meshes. We prove that this family of subspaces provides a uniformly stable discretization, see Lemma 4.6. The extension of the theory to more general discretizations is left for future work.

Let us consider a sequence of polygons $(P_N)_{N\in\mathbb{N}}$, with all of their vertices in $\partial\mathbb{D}$. We denote by h_N the maximal distance between two consecutive vertices of $\mathbb{D}_N$ and assume that

$$\lim_{N\to\infty} h_N = 0.$$

This way, the polygons P_N asymptotically cover $\mathbb{D}$. Let $\mathcal{T}_N$ be a triangulation of P_N, with the property that every vertex in the boundary of $\mathcal{T}_N$ is a vertex of P_N. For a triangle $\tau \in \mathcal{T}_N$, we denote by h_τ its diameter and by Δ_τ its area. We make the following assumptions:

$$\forall N \in \mathbb{N},\ \forall \tau \in \mathcal{T}_N, c \leq \frac{h_\tau}{h_N} \leq C \quad \text{(global quasi-uniformity)}, \tag{47}$$

$$\forall N \in \mathbb{N},\ \forall \tau \in \mathcal{T}_N, \frac{\Delta_\tau}{h_\tau^2} \geq c \qquad \text{(uniform shape-regularity)}. \tag{48}$$

Here and in what follows, $c > 0$ and $C > 0$ denote generic constants that are independent of N and of the choice of a specific triangle $\tau \in \mathcal{T}_N$. For each $N \in \mathbb{N}$, we choose $\mathcal{V}_N$ as the finite-dimensional subspace of $\widetilde{H}^{-1/2}(\mathbb{D})$ consisting of all functions $\varphi : \overline{\mathbb{D}} \to \mathbb{C}$ such that

- $\varphi_{|\tau}$ is an affine function for each $\tau \in \mathcal{T}_N$.
- φ is continuous on $\overline{P_N}$.
- φ vanishes in $\overline{\mathbb{D}} \setminus \overline{P_N}$.

To define $\mathcal{X}_N \subset \mathcal{T}^{1/2}$, we proceed as follows. If a triangle $\tau \in \mathcal{T}_N$ has two vertices A and B in $\partial\mathbb{D}$, we define U_τ as the region of $\mathbb{D}$ enclosed on the one hand by the (smallest) arc of $\partial\mathbb{D}$ linking A to B, and on the other hand by the straight line segment $[A, B]$. For each $\tau \in \mathcal{T}_N$, we then define a corresponding open set $K_\tau \subset \mathbb{D}$ by

$$\overline{K_\tau} = \begin{cases} \overline{\tau} & \text{if } \tau \text{ has at most one vertex in } \partial\mathbb{D}, \\ \overline{\tau} \cup \overline{U_\tau} & \text{otherwise.} \end{cases}$$

Hence, the domains K_τ are either triangles, or triangles with one side replaced by an arc of $\partial\mathbb{D}$. The set $\{K_\tau\}_{\tau \in \mathcal{T}_N}$ is a partition of $\mathbb{D}$, in the sense that

$$\bigcup_{\tau \in \mathcal{T}_N} \overline{K_\tau} = \overline{\mathbb{D}}.$$

With these definitions, let

$$\mathcal{X}_N := \left\{ \theta \in C^0(\overline{\mathbb{D}}) \;\middle|\; \theta_{|K_\tau} \text{ is affine for each } \tau \in \mathcal{T}_N \right\}.$$

We have $\mathcal{X}_N \subset \mathcal{T}^{1/2} = H^{1/2}(\mathbb{D})$ (while this is not true of $\mathcal{V}_N$).

For every element $\varphi \in \mathcal{V}_N$, we denote by $E_N\varphi$ the unique element of $\mathcal{X}_N$ which coincides with φ on P_N.

Lemma 4.2. *One has the estimate*

$$\forall N \in \mathbb{N},\ \forall \varphi \in \mathcal{V}_N, \quad \|\varphi - E_N\varphi\|^2_{L^2(\mathbb{D})} \leq C h_N \|\varphi\|^2_{L^2(\mathbb{D})}.$$

Proof. We start by writing

$$\|\varphi - E_N\varphi\|^2_{L^2(\mathbb{D})} = \sum_{e \in \partial\mathcal{T}_N} \int_{U_e} \left|\varphi_{|\tau(e)}(x)\right|^2 \mathrm{d}x.$$

Fix an edge $e \in \partial\mathcal{T}_N$, and let $\tau(e)$ be the triangle of $\mathcal{T}_N$ incident to e. Then $\varphi_{|\tau(e)}$ can be written in the form

$$\varphi_{|\tau(e)}(x) = \langle A, x - C \rangle + \varphi(C)$$

where C is the vertex of τ not in e and the vector A satisfies

$$\|A\|_2 \leq C h_\tau \frac{\left\|\varphi_{|\tau(e)}\right\|_\infty}{\Delta_{\tau(e)}} \leq C \frac{\left\|\varphi_{|\tau(e)}\right\|_\infty}{h_{\tau(e)}},$$

where we used the shape-regularity assumption (48). Furthermore, one has the crude estimate $\|x - C\|_2 \leq 2h_{\tau(e)}$ for $x \in U_e := K_{\tau(e)} \setminus \overline{\tau(e)}$. Hence, we conclude

$$\|\varphi - E_N\varphi\|^2_{L^2(\mathbb{D})} \leq C \sum_{e \in \partial\mathcal{T}_N} \left\|\varphi_{|\tau(e)}\right\|^2_\infty |U_e|. \tag{49}$$

We have $|U_e| \leq Ch^3_{\tau(e)}$, and, using a local inverse inequality,

$$\left\|\varphi_{|\tau(e)}\right\|^2_\infty \leq Ch^{-2}_{\tau(e)} \int_{\tau(e)} |\varphi(x)|^2 \,\mathrm{d}x.$$

Injecting those estimates in equation (49) and using the global quasi-uniformity assumption (47) gives the result. □

We have the following approximation property in $\mathcal{X}_N$.

Lemma 4.3. *For each $u \in H^{1/2}(\mathbb{D})$ and for each $N \in \mathbb{N}$, there exists $\theta \in \mathcal{X}_N$ satisfying*

$$\|u - \theta\|_{L^2(\mathbb{D})} + \sqrt{h_N}\|u - \theta\|_{H^{1/2}(\mathbb{D})} \leq C\sqrt{h_N}\|u\|_{H^{1/2}(\mathbb{D})}.$$

This result is standard for polygonal meshes, and the extension to our context, where the mesh includes some rounded triangles at the edge, presents no difficulty, so we omit the proof. The same goes for the next lemma:

Lemma 4.4. *For all $\varphi \in \mathcal{V}_N$, one has*

$$\sqrt{h_N}\|\varphi\|_{L^2(\mathbb{D})} \leq C\|\varphi\|_{\widetilde{H}^{-1/2}(\mathbb{D})},$$

and for all $\theta \in \mathcal{X}_N$, one has

$$\sqrt{h_N}\|\theta\|_{H^{1/2}(\mathbb{D})} \leq C\|\theta\|_{L^2(\mathbb{D})}.$$

By a classical argument, a global inverse inequality in combination with an approximation property ensures stability of the L^2 projection operator in the energy norm (see *e.g.* the proof of Lem. 1 from [9]). Hence

Corollary 4.5. *Let $\pi_N : L^2(\mathbb{D}) \to \mathcal{X}_N$ be the L^2 projection onto $\mathcal{X}_N$. Then there exists a constant $C_\pi > 0$ such that*

$$\forall u \in H^{1/2}(\mathbb{D}), \quad \|\pi_N u\|_{H^{1/2}(\mathbb{D})} \leq C_\pi \|u\|_{H^{1/2}(\mathbb{D})}.$$

Lemma 4.6. *There exists a constant $\sigma_0 > 0$ and an index $N_0 \in \mathbb{N}$ such that for all $N \geq N_0$,*

$$\sigma(\mathcal{V}_N, \mathcal{X}_N) \geq \sigma_0,$$

where $\sigma(\mathcal{V}_N, \mathcal{X}_N)$ is the inf-sup constant defined in equation (45).

Proof. Let $\varphi \in \mathcal{V}_N$ and let $\theta = \pi_N V\varphi$. One has $\|\theta\|_{H^{1/2}} \leq C_\pi\|\varphi\|_{\widetilde{H}^{-1/2}(\mathbb{D})}$ by Corollary 4.5. Moreover, one can write

$$\begin{aligned}\langle \varphi, \overline{\theta}\rangle &= \langle v_j, \overline{V\varphi}\rangle + \langle v_j, (I_d - \pi_N)\overline{V\varphi}\rangle \\ &= \|\varphi\|^2_{\widetilde{H}^{-1/2}} + \langle (I_d - E_N)\varphi, (I_d - \pi_N)\overline{V\varphi}\rangle,\end{aligned}$$

using the orthogonality properties of π_N. Hence, using Lemmas 4.2–4.4, we find

$$\left|\langle \varphi, \overline{\theta}\rangle\right| \geq \|\varphi\|^2_{\widetilde{H}^{-1/2}} - \sqrt{h}_N\|\varphi\|_{\widetilde{H}^{-1/2}}\|V\varphi\|_{H^{1/2}} = \left(1 - \sqrt{h_N}\right)\|\varphi\|^2_{\widetilde{H}^{-1/2}}.$$

Therefore, we have established

$$\frac{\left|\langle \varphi, \overline{\theta}\rangle\right|}{\|\varphi\|_{\widetilde{H}^{-1/2}}\|\theta\|_{H^{1/2}}} \geq \frac{1 - \sqrt{h_N}}{C_\pi}$$

which proves the lemma since $h_N \to 0$ when $N \to \infty$. □

4.4. Sesquilinear form p

We define a discrete weighted Laplacian $X_N : \mathcal{X}_N \to \mathcal{X}_N$ in the following way: for $\theta \in \mathcal{X}_N$, $X_N\theta$ is the element of $\mathcal{X}_N$ satisfying

$$\forall \theta' \in \mathcal{X}_N, \quad (X_N\theta, \theta')_{\frac{1}{\omega}} = (X\theta, \theta')_{\frac{1}{\omega}} = \frac{1}{4}\int_{\mathbb{D}} \frac{\theta(x)\overline{\theta'(x)}}{\omega(x)}\,\mathrm{d}x + \int_{\mathbb{D}} \omega(x)\nabla\theta(x)\cdot\overline{\nabla\theta'(x)}\,\mathrm{d}x.$$

This operator is self-adjoint and positive definite with respect to the scalar product $(\cdot,\cdot)_{\frac{1}{\omega}}$. For $s \in [0,1]$, let

$$\|\theta\|_{N,s}^2 := (X_N^s\theta, \theta)_{\frac{1}{\omega}}$$

which plays the role of a discrete $\mathcal{T}^s$ norm on $\mathcal{X}_N$. Let $\mathcal{X}_N^s$ denote the finite dimensional Hilbert space defined by $(\mathcal{X}_N, \|\cdot\|_{N,s})$. Reasoning with eigenfunctions of X_N in $\mathcal{X}_N$, it is easy to check that $(\mathcal{X}_N^s)_{0\le s\le 1}$ is an interpolation scale. The identity operator is continuous (with norm 1) from $\mathcal{X}_N^s$ to $\mathcal{T}^s$ for $s = 0$ and $s = 1$. By interpolation, we deduce the following estimate:

Lemma 4.7. *For all $s \in [0,1]$, there holds*

$$\forall \theta \in \mathcal{X}_N, \quad \|\theta\|_{\mathcal{T}^s} \le \|\theta\|_{N,s}.$$

On the other hand, the fact that the $\mathcal{T}^s$ norm controls the $\|\cdot\|_{N,s}$ norm can be shown by exhibiting a stable projection operator, as we show below. Here again, the argument is inspired by the proof of Lemma 1 from [9]:

Lemma 4.8. *For each $N \in \mathbb{N}$, let $\Pi_N : L^2_{\frac{1}{\omega}} \to \mathcal{X}_N$ be a linear operator satisfying the following assumptions:*

(i) $\exists C_0 > 0 : \forall N \in \mathbb{N},\ \forall u \in \mathcal{T}^0, \quad \|\Pi_N u\|_{\mathcal{T}^0} \le C_0\|u\|_{\mathcal{T}^0}$,
(ii) $\exists C_1 > 0 : \forall N \in \mathbb{N},\ \forall u \in \mathcal{T}^1, \quad \|\Pi_N u\|_{\mathcal{T}^1} \le C_1\|u\|_{\mathcal{T}^1}$,
(iii) $\forall \theta \in \mathcal{X}_N,\ \Pi_N\theta = \theta$.

Then, for all $s \in [0,1]$, there holds

$$\forall \theta \in \mathcal{X}_N, \quad \|\theta\|_{N,s} \le C_0^{1-s}C_1^s\|\theta\|_{\mathcal{T}^s}.$$

Proof. By (i) and (ii), it follow by interpolation that for all $s \in [0,1]$:

$$\forall u \in \mathcal{T}^s, \quad \|\Pi_N u\|_{N,s} \le C_0^{1-s}C_1^s\|u\|_{\mathcal{T}^s}.$$

The conclusion is immediate by restriction to $\mathcal{X}_N$, using (iii). □

It turns out that such an operator Π_N is provided by the $L^2_{\frac{1}{\omega}}$-orthogonal projection $\pi_{N,\omega}$ onto $\mathcal{X}_N$. Obviously, $\pi_{N,\omega}$ satisfies the properties (i) and (iii), while the $\mathcal{T}^1$-stability (ii) is shown in Theorem 1 of [8]. Hence, we have the following result:

Theorem 4.9. *Define the sesquilinear form p by*

$$p(\theta,\theta') := \left(X_N^{1/2}\theta, \theta'\right)_{\frac{1}{\omega}}. \tag{50}$$

Then p satisfies

$$\forall \theta \in \mathcal{X}_N \quad \|\theta\|_{\mathcal{T}^{1/2}}^2 \le p(\theta,\theta) \le C_\pi\|\theta\|_{\mathcal{T}^{1/2}}^2.$$

Gathering the previous results, we have thus established the existence of a uniform bound on the condition number of the preconditioned system $\widehat{\mathbf{P}}\mathbf{V}$, with $\widehat{\mathbf{P}}$ defined in equation (44) and p defined by equation (50).

Corollary 4.10. *There exist an index $N_0 > 0$ and a constant $\kappa_0 > 0$ such that for all $N \ge N_0$,*

$$\kappa\left(\widehat{\mathbf{P}}\mathbf{V}\right) \le \kappa_0.$$

4.5. Computation of the preconditioner

For the basis $\{\varphi_i^N\}_{1\le i\le \dim \mathcal{V}_N}$ of $\mathcal{V}_N$, we choose the classical nodal basis associated with the vertices of the triangulation $\mathcal{T}_N$. Moreover, we put

$$\theta_i^N := E_N \varphi_i^N, \quad 1 \le i \le \dim \mathcal{X}_N$$

and this in turn provides a basis for $\mathcal{X}_N$. Notice that both basis consist of real-valued functions, hence the complex conjugation is irrelevant in what follows. With those definitions, the matrix $\mathbf{D}$ is sparse and well-conditioned, so the evaluation of $\mathbf{D}^{-1}$ is cheap (in fact, $\mathbf{D}$ is nothing else than the standard mass matrix on the triangulation $\mathcal{T}_N$ of the polygonal domain P_N). To evaluate the preconditioner $\widehat{\mathbf{P}} = \mathbf{D}^{-1}\mathbf{P}\mathbf{D}^{-T}$, the main task is therefore to compute $\mathbf{P}$.

To this aim, we first remark that the matrix $\mathbf{M}_X$ of the linear operator $X_N : \mathcal{X}_N \to \mathcal{X}_N$ in the basis $\{\theta_i^N\}_{1\le i\le \dim \mathcal{X}_N}$ is given by

$$\mathbf{M}_X = \mathbf{I}_{\frac{1}{\omega}}^{-1} \mathbf{X}_{\frac{1}{\omega}}$$

where $\mathbf{I}_{\frac{1}{\omega}}$ and $\mathbf{X}_{\frac{1}{\omega}}$ are the $(\dim \mathcal{X}_N) \times (\dim \mathcal{X}_N)$ weighted "mass" and "stiffness" matrices defined by

$$\left(\mathbf{I}_{\frac{1}{\omega}}\right)_{ij} = \int_{\mathbb{D}} \frac{\theta_i^N(x)\theta_j^N(x)}{\omega(x)}\,\mathrm{d}x, \quad \left(\mathbf{X}_{\frac{1}{\omega}}\right)_{ij} := \frac{1}{4}\int_{\mathbb{D}} \frac{\theta_i^N(x)\theta_j^N(x)}{\omega(x)}\,\mathrm{d}x + \int_{\mathbb{D}} \omega(x)\nabla\theta_i^N(x)\cdot\nabla\theta_j^N(x)\,\mathrm{d}x,$$

for i, j in $\{1, \dots, \dim(\mathcal{X}_N)\}$. Those matrices can be computed using accurate quadrature rules for integrals of the form

$$\int_{K_\tau} \frac{f(x)}{\omega(x)}\,\mathrm{d}x, \quad \tau \in \mathcal{T}_N.$$

We spare the reader with the technical details about the construction of such quadratures, and instead refer to our openly available implementation [7].

The matrix $\mathbf{P}$ is equal to

$$\mathbf{P} = \mathbf{I}_{\frac{1}{\omega}} \sqrt{\mathbf{M}_X} = \mathbf{I}_{\frac{1}{\omega}} \sqrt{\mathbf{I}_{\frac{1}{\omega}}^{-1} \mathbf{X}_{\frac{1}{\omega}}}. \tag{51}$$

To evaluate the matrix square root, we use the approach of [22]. This involves a formula of the form

$$\sqrt{\mathbf{M}_X} \approx \sum_{q=1}^{Q} a_q (Id + b_q \mathbf{M}_X)^{-1} \mathbf{M}_X = \sum_{q=1}^{Q} a_q \left(\mathbf{I}_{\frac{1}{\omega}} + b_q \mathbf{X}_{\frac{1}{\omega}}\right)^{-1} \mathbf{X}_{\frac{1}{\omega}}$$

for some carefully chosen coefficients a_q and b_q, with $b_q > 0$. It is shown in [22] that, under suitable hypotheses on $\mathbf{M}_X$, the error in Froebenius norm of this approximation converges exponentially fast to 0 with respect to Q. In the end, the approximation of $\mathbf{P}$ is thus given by

$$\mathbf{P} \approx \mathbf{I}_{\frac{1}{\omega}} \sum_{q=1}^{Q} a_q \left(\mathbf{I}_{\frac{1}{\omega}} + b_q \mathbf{X}_{\frac{1}{\omega}}\right)^{-1} \mathbf{X}_{\frac{1}{\omega}}. \tag{52}$$

In all of our tests, we take $Q = 5$. The matrix $\mathbf{I}_{\frac{1}{\omega}} + b_q \mathbf{X}_{\frac{1}{\omega}}$ is sparse and symmetric positive definite. Hence, the systems

$$\left(\mathbf{I}_{\frac{1}{\omega}} + b_q \mathbf{X}_{\frac{1}{\omega}}\right) U = L$$

can be solved efficiently. Furthermore, the evaluation of the sum can be done in parallel. This allows for a cheap computation of the matrix-vector product $X \mapsto \mathbf{P}X$.

The previous subsections provide a complete description of our approach for preconditioning the Galerkin problem associated to the Laplace weakly-singular integral equation on uniform meshes. In the next sections, we indicate briefly how we tackle hypersingular equations and non-zero wavenumbers.

4.6. Extension to the hypersingular equation

Let us define

$$\mathcal{W}_N := \{\varphi \in \mathcal{V}_N \mid \varphi = 0 \text{ on } \partial\mathbb{D}_N\} \subset \widetilde{H}^{1/2}(\mathbb{D}),$$

and let $\mathcal{Y}_N := E_N\mathcal{W}_N$. Let $\{\psi_i^N\}_{1\le i\le \dim \mathcal{W}_N}$ be the nodal basis of $\mathcal{W}_N$ and let $\{\nu_i^N\}_{1\le i\le \dim \mathcal{Y}_N}$ be the basis of $\mathcal{Y}_N$ defined by

$$\nu_i^N = E_N\psi_i^N, \quad 1 \le i \le \dim \mathcal{Y}_N.$$

Let $\widetilde{\mathbf{D}}$ be the matrix of the duality pairing on $\mathcal{W}_N \times \mathcal{Y}_N$, that is

$$\widetilde{\mathbf{D}}_{ij} := \left\langle \psi_i^N, \overline{\nu_j^N} \right\rangle, \quad 1 \le i,j \le \dim \mathcal{W}_N. \tag{53}$$

Consider a well-chosen sesquilinear form $q : \mathcal{Y}_N \times \mathcal{Y}_N$, with the concrete definition given below. We then define

$$\mathbf{Q}_{ij} := q\big(\nu_i^N, \nu_j^N\big), \quad 1 \le i,j \le \dim \mathcal{Y}_N.$$

We propose to use the matrix

$$\widehat{\mathbf{Q}} := \widetilde{\mathbf{D}}^{-1}\mathbf{Q}\widetilde{\mathbf{D}}^{-T} \tag{54}$$

as a preconditioner for the Galerkin matrix $\mathbf{W}$ of the hypersingular operator on $\mathcal{W}_N$.

For the sesquilinear form q, we consider again another discrete weighted Laplacian $Y_N : \mathcal{Y}_N \to \mathcal{Y}_N$ such that for each $\nu \in \mathcal{Y}_N$, $Y_N\nu$ is the element of $\mathcal{Y}_N$ satisfying

$$\forall \nu' \in \mathcal{Y}_N, \quad (Y_N\nu, \nu)_\omega = (Y\nu, \nu')_\omega = \int_{\mathbb{D}} \frac{(\omega\nabla\omega\,\nu(x)) \cdot \overline{(\omega\nabla\omega\,\nu'(x))}}{\omega(x)}\,\mathrm{d}x.$$

Since Y_N is positive definite in the scalar product $(\cdot,\cdot)_\omega$, we may define

$$q(\nu,\nu') := \left(Y_N^{-1/2}\nu, \nu'\right)_\omega, \quad \nu,\nu' \in \mathcal{Y}_N.$$

Notice again that the matrix $\mathbf{M}_Y$ of the linear operator $Y_N : \mathcal{Y}_N \to \mathcal{Y}_N$ is given by

$$\mathbf{M}_Y = \mathbf{I}_\omega^{-1}\mathbf{Y}_\omega,$$

where $\mathbf{I}_\omega$ and $\mathbf{Y}_\omega$ are the $(\dim \mathcal{Y}_N) \times (\dim \mathcal{Y}_N)$ weighted mass and stiffness matrices defined by

$$(\mathbf{I}_\omega)_{ij} = \int_{\mathbb{D}} \omega(x)\,\nu_i^N(x)\,\nu_j^N(x)\,\mathrm{d}x, \quad (\mathbf{Y}_\omega)_{ij} := \int_{\mathbb{D}} \frac{\big(\omega\nabla\omega\,\nu_i^N(x)\big) \cdot \big(\omega\nabla\omega\,\nu_j^N\big)(x)}{\omega(x)}\,\mathrm{d}x,$$

for i,j in $\{1,\dots,\dim(Y_N)\}$. Hence, there holds

$$\mathbf{Q} = \mathbf{I}_\omega\big(\mathbf{I}_\omega^{-1}\mathbf{Y}_\omega\big)^{-1/2} = \mathbf{I}_\omega\big(\mathbf{I}_\omega^{-1}\mathbf{Y}_\omega\big)^{1/2}\big(\mathbf{I}_\omega^{-1}\mathbf{Y}_\omega\big)^{-1} = \mathbf{I}_\omega\sqrt{\mathbf{I}_\omega^{-1}\mathbf{Y}_\omega}\mathbf{Y}_\omega^{-1}\mathbf{I}_\omega. \tag{55}$$

For the efficient computation of the square root, the approach of the previous section also applies here, and leads to an approximation of the form

$$\mathbf{Q} \approx \mathbf{I}_\omega \sum_{q=1}^{Q} a_q(\mathbf{I}_\omega + b_q\mathbf{Y}_\omega)^{-1}\mathbf{I}_\omega. \tag{56}$$

4.7. Positive wavenumber

When $k > 0$, we proposed in Section 3.2 to use the operators

$$P_k = \frac{1}{\omega}\big(-\omega \operatorname{div} \omega\nabla - k^2\omega^2\big)^{\frac{1}{2}}, \quad Q_k = \omega\big(-\omega \operatorname{div} \omega\nabla - k^2\omega^2\big)^{-\frac{1}{2}},$$

as parametrices for V_k and W_k, respectively. For the Galerkin discretization, we proceed by analogy with the two previous sections. Namely, we introduce discrete weighted Laplacians $X_{k,N} : \mathcal{X}_N \to \mathcal{X}_N$ and $Y_{k,N} : \mathcal{Y}_N \to \mathcal{Y}_N$ defined by the variational problems

$$\begin{aligned} &\forall \theta, \theta' \in \mathcal{X}_N, && (X_{k,N}\theta, \theta')_{\frac{1}{\omega}} = (X_k\theta, \theta')_{\frac{1}{\omega}}, \\ &\forall \nu, \nu' \in Y_N, && (Y_{k,N}\nu, \nu')_{\omega} = (Y_k\nu, \nu')_{\omega}, \end{aligned}$$

where

$$\begin{aligned} X_k &= -\omega \operatorname{div} \omega\nabla - k^2\omega^2 - i\varepsilon(k) I_d \\ Y_k &= -\operatorname{div} \omega\nabla\omega - k^2\omega^2 - i\eta(k) I_d, \end{aligned}$$

for some functions $\varepsilon(k) > 0$ and $\eta(k) > 0$ to be specified later, where i is the imaginary unit and I_d the identity operator. In practice, this addition of a purely imaginary part to the spectrum turns out to be important for the performance of the method. The idea is borrowed from [5], where a similar approach is used to improve the approximation of a Dirichlet-to-Neumann operator in the spectral region corresponding to so-called "grazing modes" (*i.e.* $|\xi| \sim k$). This idea of "shifting" the Laplacian for preconditioning is also encountered in related contexts, see *e.g.* [16].

Clearly, $X_{k,N}$ and $Y_{k,N}$ are diagonalizable since they are the sum of a Hermitian operator (in the scalar products $(\cdot,\cdot)_{\frac{1}{\omega}}$ and $(\cdot,\cdot)_{\omega}$, respectively) and a multiple of the identity. Hence, using functional calculus, we can define $f(X_{k,N})$ and $g(Y_{k,N})$ for any well-defined functions f and g over the spectrum of $X_{k,N}$ and $Y_{k,N}$. In this sense, let

$$\begin{aligned} p_k(\theta, \theta') &:= \Big(\big(X_{k,N}\big)^{1/2}\theta, \theta'\Big)_{\frac{1}{\omega}}, && \forall (\theta, \theta') \in \mathcal{X}_N \times \mathcal{X}_N \\ q_k(\nu, \nu') &:= \Big(\big(Y_{k,N}\big)^{-1/2}\nu, \nu'\Big)_{\omega}, && \forall (\nu, \nu') \in \mathcal{Y}_N \times \mathcal{Y}_N. \end{aligned}$$

The symbol $\sqrt{\cdot}$ here stands for the principal square root, with branch cut along the negative real axis, while for any complex number $z \in \mathbb{C}$, $z^{-1/2}$ is understood as $\sqrt{z}/z$.

Let $\mathbf{P}_k$ and $\mathbf{Q}_k$ be the matrices of size $(\dim \mathcal{X}_N) \times (\dim \mathcal{X}_N)$ and $(\dim \mathcal{Y}_N) \times (\dim \mathcal{Y}_N)$ respectively, defined by

$$(\mathbf{P}_k)_{ij} := p_k\big(\theta_i^N, \theta_j^N\big), \qquad 1 \le i, j \le \dim \mathcal{X}_N, \tag{57}$$

$$(\mathbf{Q}_k)_{ij} := q_k\big(\nu_i^N, \nu_j^N\big), \qquad 1 \le i, j \le \dim \mathcal{Y}_N. \tag{58}$$

Then, we define the preconditioners

$$\widehat{\mathbf{P}}_k := \mathbf{D}^{-1}\mathbf{P}_k\mathbf{D}^{-T}, \tag{59}$$

$$\widehat{\mathbf{Q}}_k := \widetilde{\mathbf{D}}^{-T}\mathbf{Q}_k\mathbf{D}^{-1}. \tag{60}$$

The matrices $\mathbf{M}_{X,k}$ and $\mathbf{M}_{Y,k}$ of $X_{k,j}$ and $Y_{k,j}$ in the basis $\{\theta_i\}_{1 \le i \le \dim \mathcal{X}_N}$ and $\{\nu_i\}_{1 \le i \le \mathcal{Y}_N}$ are respectively given by

$$\mathbf{M}_{X,k} = \mathbf{I}_{\frac{1}{\omega}}^{-1}\Big(\mathbf{X}_{\frac{1}{\omega}} - k^2\mathbf{W}_{\frac{1}{\omega}} - i\varepsilon(k)\mathbf{I}_{\frac{1}{\omega}}\Big), \quad \mathbf{M}_{Y,k} = \mathbf{I}_{\omega}^{-1}\big(\mathbf{Y}_{\omega} - k^2\mathbf{W}_{\omega} - i\eta(k)\mathbf{I}_{\omega}\big),$$

where $\mathbf{X}_{\frac{1}{\omega}}$, $\mathbf{I}_{\frac{1}{\omega}}$, $\mathbf{X}_\omega$ and $\mathbf{I}_\omega$ are defined in the two previous subsections, and where $\mathbf{W}_{\frac{1}{\omega}}$ and $\mathbf{W}_\omega$ are respectively the $(\dim \mathcal{X}_N) \times (\dim \mathcal{X}_N)$ and $(\dim \mathcal{Y}_N) \times (\dim \mathcal{Y}_N)$ square matrices defined by

$$\left(\mathbf{W}_{\frac{1}{\omega}}\right)_{ij} = \int_{\mathbb{D}} \omega \theta_i^N(x)\theta_j^N(x)\,\mathrm{d}x, \quad (\mathbf{W}_\omega)_{ij} = \int_{\mathbb{D}} \omega(x)^3 \nu_i^N(x)\nu_j^N(x)\,\mathrm{d}x.$$

We deduce that

$$\mathbf{P}_k = \mathbf{I}_{\frac{1}{\omega}} \sqrt{\mathbf{I}_{\frac{1}{\omega}}^{-1}\left(\mathbf{X}_{\frac{1}{\omega}} - k^2 \mathbf{W}_{\frac{1}{\omega}} - i\varepsilon(k)\mathbf{I}_{\frac{1}{\omega}}\right)} = ik\mathbf{I}_{\frac{1}{\omega}} \sqrt{I_d - \mathbf{I}_{\frac{1}{\omega}}^{-1}\mathbf{A}(k)/k^2},$$

where

$$\mathbf{A}(k) = \left(\mathbf{X}_{\frac{1}{\omega}} + k^2\left(\mathbf{I}_{\frac{1}{\omega}} - \mathbf{W}_{\frac{1}{\omega}}\right) - i\varepsilon(k)\mathbf{I}_{\frac{1}{\omega}}\right).$$

To evaluate the square-root, we can no longer resort to the method of [22] since the spectrum of the matrix under the square root now occupies a region of the complex plane that is not confined to the positive real axis. We instead follow [5] and use the rational approximation of the function $X \mapsto ik\sqrt{1 - X/k^2}$ root developed in [32]. This again takes the form

$$ik\sqrt{1 - X/k^2} \approx a_0(k) + \sum_{q=1}^{Q} \frac{a_q(k)X}{1 + b_q(k)X}$$

for some explicit (complex) coefficients $a_q(k)$ and $b_q(k)$ (we use the value $\theta = \frac{\pi}{3}$, as advocated in [5], for the branch-cut rotation angle). The domain of convergence and the accuracy of this approximation is discussed in many places, for instance [30]. Choosing $\varepsilon(k) > 0$ ensures that the spectrum of $\mathbf{A}(k)$ is within the zone of convergence of this approximation. In practice, $Q = 15$ terms is more than enough in all of our tests. This leads to

$$\mathbf{P}_k \approx a_0(k)\mathbf{A}(k) + \mathbf{I}_{\frac{1}{\omega}} \sum_{q=1}^{Q} a_q(k)\left(\mathbf{I}_{\frac{1}{\omega}} + b_q(k)\mathbf{A}(k)\right)^{-1}\mathbf{A}(k). \tag{61}$$

For $\mathbf{Q}_k$, we write

$$\mathbf{Q}_k = ik\mathbf{I}_\omega(\mathbf{M}_{Y,k})^{-1}\sqrt{I_d - \mathbf{I}_\omega^{-1}\mathbf{B}(k)/k^2}$$

where

$$\mathbf{B}(k) = \mathbf{Y}_\omega + k^2(\mathbf{I}_\omega - \mathbf{W}_\omega) - i\eta(k)\mathbf{I}_\omega.$$

This leads to the approximation

$$\mathbf{Q}_k \approx \mathbf{I}_\omega\left(\mathbf{B}(k) - k^2 I_d\right)^{-1}\left\{a_0(k)\mathbf{B}(k) + \mathbf{I}_{\frac{1}{\omega}} \sum_{q=1}^{Q} a_q(k)\left(\mathbf{I}_{\frac{1}{\omega}} + b_q(k)\mathbf{B}(k)\right)^{-1}\mathbf{B}(k)\right\}. \tag{62}$$

Those approximations of $\mathbf{P}_k$ and $\mathbf{Q}_k$ have exactly the same form as equations (52) and (56), so, for the same reason, the matrix vector products $X \mapsto \mathbf{P}_k X$ and $X \mapsto \mathbf{Q}_k X$ can be evaluated cheaply. By trial and error, we have found that the functions

$$\varepsilon(k) = 0.45k, \quad \eta(k) = 0.55k$$

give good results, although, once again, we are unable to provide any theoretical foundation for those choices so far. The fact that the formulas (61) and (62) are well defined, *i.e.* that the required matrix inverses exist is also left open. This can probably be established by elementary arguments as in Lemma 8 of [3]. In our experiments, the matrices to be inverted are always fairly well-conditioned.

Remark 4.11. In principle, one can generalize the analysis to different geometries, using the same ideas as in Section 5 from [26]. That is, for a screen Γ that has a bi-Lipschitz parametrization by the unit disk $\mathbb{D}$, one may transform, *via* pullback, the integral equation on Γ into a new integral equation on $\mathbb{D}$, with a perturbed operator, which has nevertheless the same mapping properties as the usual BIOs on $\mathbb{D}$ (this follows from the L^2 and H^1 continuity of bi-Lipschitz pullbacks). The analysis then carries over without modifications.

Remark 4.12. We have chosen to discretize all operators with continuous piecewise linear functions, including the weakly singular operator V_k. In contrast, in [26], piecewise constant functions are used for the weakly singular operator, and the corresponding preconditioner is discretized over a set of piecewise linear functions on the barycentric refinement, with suitable modifications at vertices near the boundary of the screen (see Sect. 4.1.1 of the above reference).

The main reason that we see for sticking to piecewise constant functions instead of continuous piecewise linear functions is that the approximation properties of the latter in $\widetilde{H}^{-1/2}(\mathbb{D})$ have not been studied to the best of our knowledge (the standard analysis is for *discontinuous* piecewise polynomials, see *e.g.* [40]).

However, when the right-hand side of the weakly singular integral equation is smooth, which is the case *e.g.* for scattering problems, the solutions to the integral equations are in $C^\infty(\mathbb{D})$ with a square-root singularity at the edge. It is then likely that continuous linear functions do just as well as discontinuous piecewise linear functions to approximate such a density[2]. In this case, this would mean that the convergence in h of the Galerkin method is faster for piecewise linear functions than for piecewise constant functions (especially for a refined mesh, see [43], Sect. 3.2). We also note that the vector space of continuous piecewise linear functions on the screen is typically of smaller dimension than that of piecewise constant functions (as meshes of disks have about twice as many elements as vertices). With those ideas in mind, piecewise linear functions seem to be quite a good choice for discretization in practice.

5. Numerical experiments

5.1. Overview

We now present some numerical evidence to support the use of the preconditioners $\widehat{\mathbf{P}}_k$ and $\widehat{\mathbf{Q}}_k$, defined in equations (44), (59), (54) and (60), for the linear systems (37) and (38).

We present results on quasi-uniform meshes as well as on graded meshes, with a grading parameter of $\beta = 2$. For both types of meshes, we use a sequence of 9 refinement levels leading to meshes with over a million vertices. The main characteristics of those meshes are summarized in Tables 1 and 2. For the graded mesh, we report the measure in degree of the smallest angle between two edges of a triangle in the mesh. This is an indicator of the shape-regularity of this sequence of meshes. The uniform and graded meshes of levels 4 and 5 are represented in Figures 1 and 2, respectively. We remind the reader that, due to the singularity of the jumps λ and μ associated to the edge of $\mathbb{D}$, graded meshes are in theory preferable to uniform meshes in our context to speed-up the convergence of the Galerkin method [27].

To calculate the Galerkin matrices of the layer potentials, we use the Matlab toolbox GypsiLab [2]. The singular integrals are evaluated *via* semi-analytic methods. On fine meshes, the Galerkin matrices $\mathbf{V}_k$ and $\mathbf{W}_k$ do not fit in memory. In those cases, we use compression by the Fast Multipole Method (both for $k = 0$ and $k > 0$) [20,38], with the open-source Matlab wrappers of FMMLIB3D [17].

In all cases, the linear systems as well as their preconditioned versions are solved using GMRES [39], restarted every 20 iterations, with a tolerance $\varepsilon_{\text{GMRES}} = 10^{-6}$. We interrupt GMRES if it did not converge after 200 iterations (*i.e.* 10 outer iterations each consisting of 20 inner iterations). This rather low threshold allows for all the numerical tests presented below to be reproducible in around 3 days of computation.

For $k = 0$, and when the full matrices fit in memory (levels 1–4), we report the condition number κ of both the linear systems matrices and their preconditioned versions. In this case, the Galerkin matrices and their preconditioners are symmetric, so κ governs the speed of convergence of the GMRES iteration.

For large matrices (levels 5–9), computing the condition number is no longer feasible. Besides, for $k > 0$, the Galerkin matrices and their preconditioners are not normal, hence the condition number cannot be used to predict the behavior of GMRES (see *e.g.* [33]). Hence, in this case, we directly report the number of iterations needed in GMRES. The time it takes to solve iteratively the linear systems highly depends on the machine

[2]Recent papers *e.g.* [44] have emphasized the role of *broken Bramble–Hilbert lemmas* to prove that continuous Lagrange piecewise polynomials have the same approximation power as discontinuous ones. This analysis is only available for second order elliptic PDEs for now.

TABLE 1. Characteristics of the uniform meshes used in the experiments. The parameter $h_{\min}$ (resp. $h_{\max}$) is the length of the shortest (resp. longest) edge in the mesh.

Refinement level	$h_{\max}$	$h_{\min}$	Number of vertices	Number of triangles
1	0.47	0.29	40	59
2	0.23	0.14	136	232
3	0.13	0.079	421	770
4	0.067	0.041	1462	2790
5	0.034	0.021	5431	10 602
6	0.017	0.011	20 907	41 303
7	8.7e−3	5.4e−3	83 038	165 056
8	4.4e−3	2.7e−3	328,935	655 838
9	2.2e−3	1.3e−3	1 313 387	2 622 713

TABLE 2. Characteristics of the graded meshes used in the experiments. The parameter $h_{\min}$ (resp. $h_{\max}$) is the length of the shortest (resp. longest) edge in the mesh, while $\theta_{\min}$ is the measure in degrees of the smallest angle between two edges of a triangle of the mesh.

Refinement level	$h_{\max}$	$h_{\min}$	$\theta_{\min}$	Number of vertices	Number of triangles
1	0.75	0.25	9.0	32	37
2	0.47	0.0625	8.4	153	204
3	0.34	0.020	8.2	541	773
4	0.21	6.9e−3	8.2	1815	2724
5	0.11	2.1e−3	8.2	6983	10 923
6	0.068	6.25e−4	8.2	26 000	41 945
7	0.037	1.8e−4	8.2	99 418	164 428
8	0.020	5.3e−5	8.2	376 760	635 589
9	0.011	1.5e−05	8.2	1 455 784	2 496 568

used for the calculations. Nevertheless, we still report timings for our machine in order to give a rough idea of the speedups that can be expected when using our method. When GMRES does not reach the tolerance after 200 iterations, we report the time taken to perform those 200 iterations, although the system should not be considered as being solved. All floating point numbers are rounded to 2 significant digits.

When the full matrices fit in memory, the computation of the matrix square roots are done using the Matlab function `sqrtm`. For larger matrices and when $k = 0$, we use the approximations (52) and (56) based on [22]. For $k > 0$, we use instead the approximations (61) and (62) based on the rational approximation of $X \mapsto ik\sqrt{1 - X/k^2}$ from [32].

For the matrix $\mathbf{W}_k$, we compare the performance of our square-root preconditioner with the Calderón preconditioner [11][3]

$$\widehat{\mathbf{C}}_k := \widetilde{\mathbf{D}}^{-T}\widetilde{\mathbf{V}}_k\widetilde{\mathbf{D}}^{-1}, \tag{63}$$

where $\widetilde{\mathbf{V}}_k$ is the Galerkin matrix of the weakly singular operator over the space $\mathcal{W}_N$, that is, the space of piecewise linear elements on the triangulation $\mathcal{T}_N$ with Dirichlet conditions on $\partial\mathcal{T}_N$. The Calderón preconditioner turns out to be particularly efficient in our tests, probably due to the fact that the screen $\mathbb{D}$ is flat. Indeed, because of this, the double layer potential vanishes on $\mathbb{D}$, so that, sloppily speaking, *i.e.* pretending that $\mathbb{D}$ were a smooth

[3]We could also consider a Calderón preconditioner for $\mathbf{V}_k$, but this is slightly less straightforward, since W has a non-trivial kernel on the finite-element space of piecewise linear functions with no Dirichlet conditions on $\partial\mathbb{D}$.

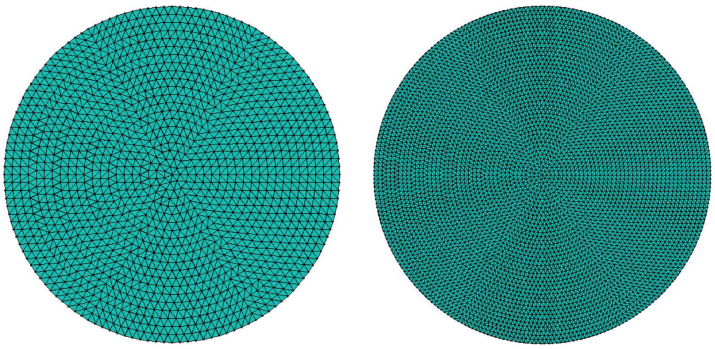

FIGURE 1. Uniform meshes of levels $n = 4$ (*left*) and $n = 5$ (*right*).

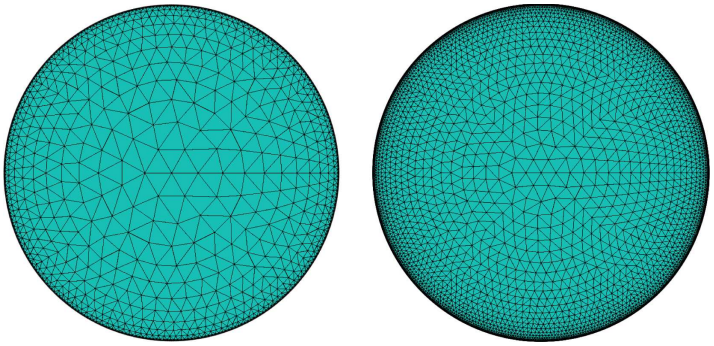

FIGURE 2. Non-uniform meshes of levels $n = 5$ (*left*) and $n = 6$ (*right*).

closed surface in $\mathbb{R}^3$, the Calderón formula ([34], Thm. 3.1.3) would read

$$V_k W_k = W_k V_k = \frac{1}{4} I_d.$$

5.2. Results

We now report and discuss our numerical results. They are obtained on a computer running on 8 cores with multi-threading, with a clock rate of 3.8 GHz, and with 32 GB of RAM.

Laplace equation on uniform meshes

In Tables 3 and 4 below, we report the performance of $\widehat{\mathbf{P}}$ as a preconditioner for $\mathbf{V}$ on a sequence of uniform meshes.

Results for the Laplace hypersingular equation on uniform meshes are reported in Tables 5 and 6.

Those results confirm the expectations that $\widehat{\mathbf{P}}$ and $\widehat{\mathbf{Q}}$ are excellent preconditioners for $\mathbf{V}$ and $\mathbf{W}$ on uniform meshes. For levels 1–4, they lead to condition numbers below 2, and for levels 5–9, the number of GMRES iterations required to reach the tolerance never exceeds 7. Table 5 highlights the difference with the Calderon preconditioner $\widehat{\mathbf{C}}$, which is known to suffer form the so-called "duality mismatch" (the fact that $H^{1/2}(\mathbb{D})$ and $H^{-1/2}(\mathbb{D})$ are not dual to each other). This property translates into a slow increase in the condition number, see *e.g.* [41], Proposition 3 of [11]. Despite this, the resolution time with the Calderón preconditioner is roughly similar to that of our square-root preconditioners in our setting, with a slight advantage for the former.

TABLE 3. Condition numbers of the matrices $\mathbf{V}$, $\mathbf{D}^{-1}\mathbf{V}$ (mass matrix preconditioner) and $\widehat{\mathbf{P}}\mathbf{V}$ (square-root preconditioner) assembled on uniform meshes.

Refinement level	$\kappa(\mathbf{V})$	$\kappa(\mathbf{D}^{-1}\mathbf{V})$	$\kappa(\widehat{P}\mathbf{V})$
1	82.9215	13.1953	1.3956
2	184.2518	26.3687	1.411
3	355.0135	48.6967	1.4514
4	686.7896	93.3797	1.4814

TABLE 4. Number of iterations n and time t in seconds needed for the iterative resolution of the hypersingular equation (37) for $k = 0$, on uniform meshes, with the right-hand side F_N corresponding to the function $f(x) = 1/\omega(x)$ in equation (41). Columns 2–3 and 4–5 correspond to the resolution without preconditioner, and with our square-root preconditioner $\widehat{\mathbf{P}}$, respectively.

Refinement level	No prec.		Square-root prec.	
	n	t	n	t
5	128	9.0	6	2.0
6	>200	45	6	6.0
7	>200	180	6	26
8	>200	730	6	130
9	>200	2.9e3	7	785

TABLE 5. Condition numbers of the matrices $\mathbf{W}$, $\widehat{\mathbf{C}}\mathbf{W}$ (Calderón preconditioner) and $\widehat{\mathbf{Q}}\mathbf{W}$ (square-root preconditioner), assembled on uniform meshes.

Refinement level	$\kappa(\mathbf{W})$	$\kappa\left(\tilde{\mathbf{D}}^{-1}\mathbf{W}\right)$	$\kappa\left(\widehat{C}\mathbf{W}\right)$	$\kappa\left(\widehat{Q}\mathbf{W}\right)$
1	2.4226	6.5229	1.8971	1.3051
2	4.5353	13.8201	2.4223	1.4149
3	8.3698	25.5514	3.1051	1.488
4	16.0808	49.177	4.2366	1.5601

Laplace equation on graded meshes

We report in Tables 7 and 8 the preconditioning performance for the weakly singular operator on graded meshes.

From those results, it seems that a result such as Theorem 4.1 is not verified on our sequence of graded meshes, as the condition number of $\widehat{\mathbf{P}}\mathbf{V}$ now seems to increase with mesh refinement. The condition number improvement nevertheless remains drastic, and the number of GMRES iterations required to solve the system on finer levels remains small, as shown in Table 8.

Notice that without preconditioner, the desired tolerance is never reached with 200 iterations. The weakly singular operator is so ill-conditioned on the graded meshes that the GMRES residuals almost stagnate. On the finest levels, the required number of iterations is probably much larger than 200, so the speedup allowed by our preconditioners is underestimated by the figures of Table 8.

TABLE 6. Number of iterations n and time t in seconds needed for the iterative resolution of the hypersingular equation (38) for $k = 0$, on uniform meshes, with the right-hand side G_N corresponding to the function $g(x) = \omega(x)$ in equation (41). Columns 2–3, 4–5 and 6–7 correspond to the resolution without preconditioner, with the Calderón preconditioner $\widehat{\mathbf{C}}$, and with our square-root preconditioner $\widehat{\mathbf{Q}}$, respectively.

Refinement level	No prec.		Calderón prec.		Square-root prec.	
	n	t	n	t	n	t
5	22	3.4	7	2.2	5	2.2
6	30	15	6	6.8	5	6.8
7	57	110	6	29	5	29
8	107	850	7	140	5	140
9	183	6.0e3	7	650	5	740

TABLE 7. Condition numbers or the matrices $\mathbf{V}$, $\mathbf{D}^{-1}\mathbf{V}$ (mass-matrix preconditioner), and $\widehat{\mathbf{P}}\mathbf{V}$ (square-root preconditioner) assembled on graded meshes.

Refinement level	$\kappa(\mathbf{V})$	$\kappa\left(\mathbf{D}^{-1}\mathbf{V}\right)$	$\kappa\left(\widehat{P}\mathbf{V}\right)$
1	700	20	2.4
2	1.6e4	99	3.2
3	1.7e5	330	4.8
4	1.5e6	1.0e3	9.6

TABLE 8. Number of iterations n and resolution time t in seconds for the iterative resolution of the weakly singular equation (37) for $k = 0$ on graded meshes, with the right-hand side F_N corresponding to the function $f(x) = 1/\omega(x)$ in equation (41). Columns 2–3 and 4–5 correspond to the resolution without preconditioner, and with our square-root preconditioner $\widehat{\mathbf{P}}$, respectively.

Refinement level	No prec.		Square-root prec.	
	n	t	n	t
5	>200	14	7	2.3
6	>200	50	8	7.1
7	>200	200	8	28
8	>200	750	8	120
9	>200	3.1e3	8	530

In Tables 9 and 10, we report the results concerning the hypersingular operator.

In contrast to the case of the weakly-singular equation, the preconditioner $\hat{Q}$ seems to lead to a uniformly bounded condition number even on graded meshes. The difference with the Calderón is again noticeable, and this time, it is also reflected in the resolution time. On the finest graded mesh, the square-root preconditioner speeds up the resolution by a factor 2 compared to the Calderón preconditioner, and allows to solve a problem on a mesh with 2.5 millions of elements in less than 10 min (while almost 2 h without preconditioner weren't enough to reach the desired tolerance).

TABLE 9. Condition numbers or the matrices $\mathbf{W}$, $\widehat{\mathbf{C}}\mathbf{W}$ (Calderón preconditioner), and $\widehat{\mathbf{Q}}\mathbf{W}$ (square-root preconditioner) assembled on graded meshes.

Refinement level	$\kappa(\mathbf{W})$	$\kappa\left(\widehat{Q}\mathbf{W}\right)$	$\kappa\left(\widehat{C}\mathbf{W}\right)$
1	1.4	1.2	1.7
2	3.3	1.3	2.5
3	7.45	1.4	3.3
4	15	1.4	4.1

TABLE 10. Number of iterations n and time t in seconds needed for the iterative resolution of the hypersingular equation (38) for $k = 0$, on graded meshes, with the rhs G_N corresponding to the function $g(x) = \omega(x)$ in equation (41). Columns 2–3, 4–5 and 6–7 correspond to the resolution without preconditioner, with the Calderón preconditioner $\hat{C}$, and with our square-root preconditioner $\hat{Q}$, respectively.

Refinement level	No prec.		Calderón prec.		Square-root prec.	
	n	t	n	t	n	t
5	38	5.6	9	2.5	5	2.0
6	58	31.7	10	10	5	6.0
7	86	180	10	41	5	24
8	131	1.1e3	11	180	5	100
9	>200	6.5e3	12	820	5	430

TABLE 11. Number of iterations n and resolution time t in seconds for the iterative resolution of the weakly singular equation (37) on uniform meshes, with the right-hand side F_N corresponding to the Dirichlet trace of the plane wave (64). Columns 2–3 and 4–5 correspond to the resolution without preconditioner, and with our square-root preconditioner $\widehat{\mathbf{P}}_k$, respectively.

Refinement level	k	No prec.		Square-root prec.	
		n_1	t_1	n_2	t_2
1	1.1	20	0.1	8	0.8
2	2.1	40	0.43	8	1.2
3	3.9	69	1.45	7	1.4
4	7.4	124	8.4	8	2.3
5	14.5	167	47	8	5.6
6	29	>200	220	7	19.2
7	57	>200	900	7	85.5
8	115	>200	3.65e3	8	488
9	228	>200	1.5e4	10	3.55e3

TABLE 12. Number of iterations n and resolution time t in seconds for the iterative resolution of the hypersingular equation (38) on uniform meshes, with the right-hand side G_N corresponding to the Neumann trace of the plane wave (64). Columns 2–3, 4–5 and 6–7 correspond to the resolution without preconditioner, with the Calderón preconditioner $\widehat{\mathbf{C}}_k$ and with our square-root preconditioner $\widehat{\mathbf{Q}}_k$, respectively.

Refinement level	k	No prec.		Square-root prec.		Calderón prec.	
		n_1	t_1	n_2	t_2	n_3	t_3
1	1.1	7	0.1	6	0.8	6	0.1
2	2.1	11	0.4	6	1.2	7	0.4
3	3.9	20	1.3	7	1.7	8	0.8
4	7.4	43	8.9	7	3.3	9	2.9
5	14.5	51	44	7	9.9	8	11
6	29	59	200	7	38.5	8	44
7	57	69	950	8	190	7	162
8	115	81	4.5e3	9	985	7	670
9	228	94	2.1e4	12	6.4e3	7	2.8e3

Helmholtz equation on uniform meshes

We now turn our attention to the case of a non-zero wavenumber $k > 0$. In what follows, we have chosen $k = 1/(2h_{\max})$ for the uniform meshes, and $k = 1/h_{\max}$ for the graded meshes, where $h_{\max}$ is the length of the longest edge in the mesh. With those choices, the mesh accurately represents the wavelengths as small as $2\pi/k$. In Table 11 below, we report the preconditioning performance for the weakly singular operator. We consider the scattering by $\mathbb{D}$ of a plane wave of wavenumber k illuminating the disk with an angle $\pi/4$ with respect to the vertical axis. In other words, the right-hand sides of equations (37) and (38) are chosen as Dirichlet and Neumann traces, respectively, of the plane wave

$$\forall x \in \mathbb{R}^3, \quad u_{\text{inc}}(x) := e^{ik\frac{x_1+x_3}{\sqrt{2}}}. \tag{64}$$

We report the results on uniform meshes in Table 11 (weakly-singular operator) and Table 12 (hypersingular operator) below.

The results of this section demonstrate the robustness of our preconditioners with respect to the wavenumber on uniform meshes. However, in Table 12, we see that the Calderón preconditioner still performs better than our square-root preconditioner, both from the point of view of resolution time and number of iterations.

Helmholtz equation on uniform meshes

We now report results for the Helmholtz equation on graded meshes (Tabs. 13 and 14).

The performance of our preconditioners on graded meshes seems to be even better than on uniform meshes. In this case, our square-root preconditioner outperforms the Calderón preconditioner.

Different corrections

Finally, we would like to illustrate the practical importance of the corrective term $-k^2\omega^2$ in the definitions P_k and Q_k. For this, we compare our preconditioner P_k with three alternatives. The first one is $\widehat{\mathbf{P}}$ (the preconditioner used for $k = 0$). The second and third ones are based on the operators

$$T_k := \frac{1}{\omega}\left(-\omega \operatorname{div} \omega\nabla - k^2\mathrm{Id}\right)^{\frac{1}{2}}, \quad \Lambda_k := \left(-\Delta - k^2\mathrm{Id}\right)^{\frac{1}{2}} \tag{65}$$

TABLE 13. Number of iterations n and resolution time t in seconds for the iterative resolution of the weakly singular equation (37) on graded meshes, with the right-hand side F_N corresponding to the Dirichlet trace of the plane wave (64). Columns 2–3 and 4–5 correspond to the resolution without preconditioner, and with our square-root preconditioner $\widehat{\mathbf{P}}_k$, respectively.

Refinement level	k	No prec.		Square-root prec.	
		n	t	n	t
1	1.3	17	0.1	8	0.8
2	2.1	>200	1.3	8	0.9
3	2.9	>200	4.0	8	1.5
4	4.7	>200	9.4	8	2.2
5	8.5	>200	41	8	4.6
6	15	>200	160	8	16
7	27	>200	630	8	64
8	50	>200	2.4e3	8	280
9	91	>200	9.5e3	9	1.3e3

TABLE 14. Number of iterations n and resolution time t in seconds for the iterative resolution of the hypersingular equation (38) on graded meshes, with the rhs G_N corresponding to the Neumann trace of the plane wave (64). Columns 2–3, 4–5 and 6–7 correspond to the resolution without preconditioner, with the Calderón preconditioner $\widehat{\mathbf{C}}_k$ and with our square-root preconditioner $\widehat{\mathbf{Q}}_k$, respectively.

Refinement level	k	No prec.		Calderón prec.		Square-root prec.	
		n	t	n	t	n	t
1	1.3	5	0.1	4	0.1	5	0.6
2	2.1	12	0.1	8	0.3	6	0.9
3	2.9	20	1.0	9	0.9	6	1.6
4	4.7	36	5.0	11	2.4	6	2.4
5	8.5	84	51	11	10	7	7.4
6	15	137	320	12	43	7	26
7	27	>200	1.9e3	12	170	7	110
8	50	>200	7.2e3	12	670	8	480
9	91	>200	2.9e4	12	2.7e3	9	2.3e3

The operators T_k and Λ_k are converted into preconditioners $\widehat{\mathbf{T}}_k$ and $\widehat{\Lambda}_k$ for $\mathbf{V}_k$ in the same way as $\widehat{\mathbf{P}}_k$ is derived from $\mathbf{P}_k$, see Section 4. Using $\widehat{\mathbf{P}}$ in place of $\widehat{\mathbf{P}}_k$ amounts to ignoring the k-dependency of $\mathbf{V}_k$. The preconditioner $\widehat{\mathbf{T}}_k$ is a naive attempt to include a k-dependency in the preconditioner. Finally, the preconditioner $\widehat{\Lambda}_k$ corresponds to the approximation of the DtN map from [5] for a smooth surface. Using this preconditioner amounts to ignoring the edge singularity of the screen by formally putting $\omega \equiv 1$.

We report the performance of those preconditioners on uniform and graded meshes in Table 15.

The results clearly show that, among other attempts, our square-root preconditioner is the most robust both to the increase of the condition number and to mesh grading.

TABLE 15. Number of iterations n for the iterative resolution of the weakly-singular equation (38) on uniform meshes (left) and graded meshes (right), with the right-hand side F_N corresponding to the Dirichlet trace of the plane wave (64). In each table, columns 3, 4, 5 and 6 correspond to the resolution with the preconditioners, $\widehat{\mathbf{P}}_k$, $\widehat{\mathbf{P}}$, $\widehat{\mathbf{T}}_k$ and $\widehat{\Lambda}_k$, respectively.

Uniform meshes

		$\widehat{\mathbf{P}}_k$	$\widehat{\mathbf{P}}$	$\widehat{\mathbf{T}}_k$	$\widehat{\Lambda}_k$
Level	k	n	n	n	n
1	1.1	8	7	10	10
2	2.1	8	8	15	11
3	3.9	7	11	26	12
4	7.4	8	21	44	13
5	14.5	8	51	68	15
6	29	7	87	95	17
7	57	7	157	128	20
8	115	8	>200	152	25

Graded meshes

		$\widehat{\mathbf{P}}_k$	$\widehat{\mathbf{P}}$	$\widehat{\mathbf{T}}_k$	$\widehat{\Lambda}_k$
Level	k	n	n	n	n
1	1.3	8	8	10	10
2	2.1	8	10	16	15
3	2.9	8	11	20	19
4	4.7	8	14	30	28
5	8.5	8	35	51	38
6	15	8	53	78	56
7	27	8	99	116	89
8	50	8	163	>200	143

APPENDIX A. PROOF OF THEOREM 2.13

We remark that the identity on associated Legendre polynomials P_l^m (see [1], Eq. (8.5.3))

$$\forall t \in \mathbb{R}, \quad tP_l^m(t) = \frac{1}{(2l+1)}\big((l+1-m)P_{l+1}^m(t) + (l+m)P_{l-1}^m(t)\big),$$

permits us to deduce a simple algebraic property that connects the functions (T_l^m) and (U_l^m).

Lemma A.1. *For all $(l,m) \in \Lambda$ there holds*

$$T_l^m = j_{l+1}^m U_l^m + j_l^m U_{l-2}^m \tag{A.1}$$

$$U_l^m = \frac{j_{l+2}^m T_{l+2}^m + j_{l+1}^m T_l^m}{\omega^2} \tag{A.2}$$

where

$$j_l^m = \begin{cases} 0 & \text{if } l = 0, \\ \sqrt{\dfrac{l^2-m^2}{4l^2-1}} & \text{otherwise,} \end{cases} \tag{A.3}$$

and taking the convention $U_{-2}^m = U_{-1}^m = 0$ in equation (A.1).

We omit the proof of this lemma which is a simple calculation. We deduce

Lemma A.2. *For all $s \geq 0$, $\mathcal{T}^s$ is continuously embedded in $\mathcal{U}^s$.*

Proof. We define a map $I : \mathcal{T} \to \mathcal{U}$ by

$$I\left(\sum_{(l,m)\in\Lambda} \hat{u}_l^m T_l^m\right) = \sum_{(l,m)\in\Lambda} \big(j_{l+1}^m \hat{u}_l^m + j_{l+2}^m \hat{u}_{l+2}^m\big) U_l^m,$$

with the coefficients j_l^m given in equation (A.3). The map I is continuous from $\mathcal{T}^s$ to $\mathcal{U}^s$ for all $s \in \mathbb{R}$ since for all $(l,m) \in \Lambda$, one has $|j_l^m| \leq 1$. Moreover, by equation (A.1), I coincides with the identity operator $\mathrm{Id} : L^2_{\frac{1}{\omega}} \to L^2_\omega$ on the dense subset of $L^2_{\frac{1}{\omega}}$ consisting of finite linear combinations of the functions $\{T_l^m\}_{(l,m)\in\Lambda}$. Hence, $Iu = u$ for all $u \in L^2_{\frac{1}{\omega}} \supset \mathcal{T}^s$, and the result follows. □

Next, we establish continuous inclusions $\mathcal{U}^s \subset \mathcal{T}^{s-1}$ for $s \geq 1$. This turns out to be more delicate: roughly speaking, we need to proceed to the inversion of the formula (A.1) expressing T_l^m in terms of U_l^m and U_{l-2}^m, with careful estimation of the underlying coefficients. We start with the following technical lemma:

Lemma A.3. (1) *Let $(l,m) \in \Lambda$. Then*

$$U_l^m = \sum_{\substack{k=|m| \\ l-k \text{ even}}}^{l} (-1)^{\frac{l-k}{2}} \kappa_{l,m,k} T_k^m \tag{A.4}$$

where the coefficients $\kappa_{l,m,k}$ are defined whenever $|m| \leq k \leq l$ and l, k and m all share the same parity, as follows.

- *For all $(l,m) \in \Lambda$,*

$$\kappa_{l,m,l} = \frac{1}{j_{l+1}^m}. \tag{A.5}$$

- *For all $|m| \leq k \leq l$ such that k, l and m have the same parity,*

$$\kappa_{l+2,m,k} = \frac{j_{l+2}^m}{j_{l+3}^m} \kappa_{l,m,k}. \tag{A.6}$$

Thus,

$$\kappa_{l,m,k} = \left(\prod_{\substack{\nu=k+2 \\ l-\nu \text{ even}}}^{l} j_\nu^m \right) \left(\prod_{\substack{\nu=k \\ l-\nu \text{ even}}}^{l} j_{\nu+1}^m \right)^{-1}. \tag{A.7}$$

(2) *For all $|m| \leq k \leq l-2$ with k, l, m of the same parity, there holds*

$$\kappa_{l,m,k} = \frac{j_{k+2}^m}{j_{k+1}^m} \kappa_{l,m,k+2}. \tag{A.8}$$

(3) *These coefficients satisfy*

$$\kappa_{l,m,k} \leq \begin{cases} \frac{1}{j_{k+1}^m} & \text{if } m \neq 0, \\ 2 & \text{if } m = 0. \end{cases}$$

Proof. The formula (A.4) is readily obtained by induction by combining equation (A.1) with equations (A.5) and (A.6). The formula (A.7) can be easily proven by induction from equations (A.5) and (A.6). From (A.7), (A.8) follows immediately. Then, writing

$$\begin{aligned} \left(j_{l+1}^m\right)^2 &= \frac{(l+1)^2 - m^2}{(2l+1)(2l+3)} \\ &= \frac{1}{4} + \left(\frac{1}{4} - m^2\right) \frac{1}{(2l+1)(2l+3)} \end{aligned}$$

defined when $(l+1) \geq |m|$, we notice that for $m \neq 0$ (resp. $m = 0$), the sequence $(j_{l+1}^m)_l$ increases (resp. decreases) with respect to l. We deduce, since

$$\frac{\kappa_{l+2,m,k}}{\kappa_{l,m,k}} = \frac{j_{l+2}^m}{j_{l+3}^m},$$

that for $m \neq 0$, the sequence $(\kappa_{l,m,k})_l$ decreases with respect to l, and thus

$$\kappa_{l,m,k} \leq \kappa_{k,m,k} = \frac{1}{j^m_{k+1}}.$$

For $m = 0$, we can write

$$\kappa_{l,0,k} = \frac{1}{j^0_{l+1}} \left(\frac{j^0_l}{j^0_{l-1}} \right) \cdots \left(\frac{j^0_{k+2}}{j^0_{k+1}} \right) \leq \frac{1}{j^0_{l+1}} \leq \lim_{l \to \infty} \frac{1}{j^0_{l+1}} = 2.$$

□

We further need two intermediate results. The first is a more explicit estimate of $\kappa_{l,m,k}$ presented in the following lemma.

Lemma A.4. *For all integers such that $\kappa_{l,m,k}$ is defined, there holds*

$$\kappa_{l,m,k} \leq 2 \frac{\sqrt{(l+1)(l+2) - m^2}}{l + 1 - |m|}. \tag{A.9}$$

Proof. Only the case $m \neq 0$ deserves attention. By Lemma A.3 above, $\kappa_{l,m,k} \leq \frac{1}{j^m_{k+1}} \leq \frac{1}{j^m_{l+1}}$ since j^m_l is increasing with respect to l. We then write

$$\frac{1}{j^m_{l+1}} = \sqrt{\frac{(2l+1)(2l+3)}{(l+1)^2 - m^2}} \leq \frac{2(l+1)\sqrt{(l+1)^2 - m^2}}{(l+1)^2 - m^2} \leq 2 \frac{\sqrt{(l+1)^2 - m^2}}{l + 1 - |m|}$$

from which (A.9) follows. □

Second, we need an adjoint Cesarò estimate. It is well-known that the Cesarò operator K defined for $v \in l^2(\mathbb{N}^*)$ by

$$(Kv)_n = \frac{1}{n} \sum_{k=1}^{n} v_k,$$

is continuous in $l^2(\mathbb{N}^*)$. Therefore, its adjoint K^*, defined by

$$(K^* v)_n = \sum_{k=n}^{+\infty} \frac{v_k}{k},$$

is also continuous. Hence, there exists a constant $C_K > 0$ such that for all $v \in l^2(\mathbb{N})$, there holds

$$\sum_{n=1}^{+\infty} \left| \sum_{k=n}^{+\infty} \frac{v_k}{k} \right|^2 \leq C_K \|v\|^2_{l^2}.$$

Here we rewrite this inequality for sequences v of the form $(v_l)_{l \geq |m|}$. In this case, one can check by manipulations on the indices that the previous implies

$$\sum_{l=|m|}^{+\infty} \left| \sum_{k=l}^{+\infty} \frac{v_k}{k + 1 - |m|} \right|^2 \leq C'_K \sum_{l=|m|}^{+\infty} |v_l|^2 \tag{A.10}$$

for some constant $C'_K > 0$ independent of m. We are now in a position to prove the inclusion of $\mathcal{U}^s$ into $\mathcal{T}^{s-1}$ for $s \geq 1$:

Lemma A.5. *For all $s \geq 1$, $\mathcal{U}^s$ is continuously embedded in $\mathcal{T}^{s-1}$.*

Proof. Let $s > \frac{1}{2}$. To $u \in \mathcal{U}^s$ given by

$$u = \sum_{(l,m)\in\Lambda} \beta_l^m U_l^m,$$

we associate the element $\widetilde{I}u$ of $\mathcal{T}$ defined by

$$\widetilde{I}u := \sum_{(l,m)\in\Lambda} \alpha_l^m T_l^m,$$

where

$$\alpha_k^m = \sum_{\substack{l=k \\ l-k \text{ even}}}^{+\infty} (-1)^{\frac{l-k}{2}} \kappa_{l,m,k} \beta_l^m. \tag{A.11}$$

We claim that for all $s > \frac{1}{2}$, $\widetilde{I}$ maps $\mathcal{U}^s$ to $\mathcal{T}^{s-1}$ continuously and satisfies

$$\forall u \in \mathcal{U}^s, \quad I\widetilde{I}u = u, \tag{A.12}$$

where I is the operator defined in Lemma A.2.

Firstly, the sum on the rhs of equation (A.11) converges absolutely for $s > \frac{1}{2}$. Indeed, applying Lemma A.3 and the Cauchy–Schwarz inequality, we have

$$\sum_{\substack{l=k \\ l-k \text{ even}}}^{+\infty} \left|(-1)^{\frac{l-k}{2}} \kappa_{l,m,k} \beta_l^m\right| \leq \frac{1}{j_{k+1}^m} \sqrt{\sum_{\substack{l=|m| \\ l-m \text{ even}}}^{+\infty} [(l+1)(l+2) - m^2]^s |\beta_l^m|^2} \sqrt{\sum_{\substack{l=|m| \\ l-m \text{ even}}}^{+\infty} [(l+1)(l+2) - m^2]^{-s}}.$$

The first sum is $\|u\|_{\mathcal{U}^s}$, and the second one is finite for $s > \frac{1}{2}$. This shows that $\widetilde{I}u$ is well-defined.

Secondly, one has for all $(k,m) \in \Lambda$,

$$\begin{aligned} j_{k+1}^m \alpha_k^m + j_{k+2}^m \alpha_{k+2}^m &= j_{k+1}^m \left(\sum_{\substack{l=k \\ l-k \text{ even}}}^{+\infty} (-1)^{\frac{l-k}{2}} \kappa_{l,m,k} \beta_l^m \right) + j_{k+2}^m \left(\sum_{\substack{l=k+2 \\ l-k \text{ even}}}^{+\infty} (-1)^{\frac{l-k-2}{2}} \kappa_{l,m,k+2} \beta_l^m \right) \\ &= j_{k+1}^m \kappa_{k,m,k} \beta_k^m + \sum_{\substack{l=k+2 \\ k-l \text{ even}}}^{+\infty} (-1)^{\frac{(l-k)}{2}} \left[j_{k+1}^m \kappa_{l,m,k} - j_{k+2}^m \kappa_{l,m,k+2} \right] \beta_l^m \\ &= \beta_k^m \end{aligned}$$

using equation (A.8) and the definition of $\kappa_{k,m,k}$. This proves the identity (A.12).

Finally, we write

$$\begin{aligned} \left\|\widetilde{I}u\right\|_{\mathcal{T}^{s-1}}^2 &= \sum_{m=0}^{+\infty} \sum_{\substack{l=|m| \\ l-m \text{ even}}}^{+\infty} \left(\frac{1}{4} + l(l+1) - m^2\right)^{s-1} |\alpha_l^m|^2 \\ &= \sum_{m=0}^{+\infty} \sum_{\substack{l=|m| \\ l-m \text{ even}}}^{+\infty} \left(\frac{1}{4} + l(l+1) - m^2\right)^{s-1} \left| \sum_{\substack{k=l \\ k-l \text{ even}}}^{+\infty} (-1)^{\frac{k-l}{2}} \kappa_{k,m,l} \beta_k^m \right|^2 \end{aligned}$$

$$\leq 4\sum_{m=0}^{+\infty}\sum_{\substack{l=|m|\\ l-m \text{ even}}}^{+\infty}\left(\sum_{\substack{k=l\\ k-l \text{ even}}}^{+\infty}\left((k+1)(k+2)-m^2\right)^{\frac{s-1}{2}}\frac{\sqrt{(k+1)(k+2)-m^2}}{k+1-|m|}|\beta_k^m|\right)^2$$

using the inequality (A.9) and the simple estimate

$$\frac{1}{4}+l(l+1)-m^2\leq (l+1)(l+2)-m^2\leq (k+1)(k+2)-m^2$$

valid for $l\leq k$. We deduce

$$\begin{aligned}\left\|\widetilde{I}u\right\|_{\mathcal{T}^{s-1}}^2 &\leq 4\sum_{m=0}^{+\infty}\sum_{\substack{l=|m|\\ l-m \text{ even}}}^{+\infty}\left|\sum_{\substack{k=l\\ k-l \text{ even}}}^{+\infty}\left((k+1)(k+2)-m^2\right)^{\frac{s}{2}}\frac{|\beta_k^m|}{k+1-|m|}\right|^2\\ &\leq 4C_K'\sum_{m=0}^{+\infty}\sum_{\substack{l=|m|\\ l-m \text{ even}}}^{+\infty}\left[(l+1)(l+2)-m^2\right]^s|\beta_l^m|^2\\ &= 4C_K'\|u\|_{\mathcal{U}^s}^2\end{aligned}$$

where we applied the adjoint Cesarò estimate (A.10) with $v_k=((k+1)(k+2)-m^2)^{\frac{s}{2}}|\beta_l^m|$. This proves the claimed continuity.

For $s\geq 1$, we have shown in Lemma A.2 that I coincides with Id on $\mathcal{T}^{s-1}$. Thus, equation (A.12) states nothing else than

$$\widetilde{I}u=u,$$

and the lemma is proved. □

Remark A.6. At this point, it is looks very natural to identify an element $u\in\mathcal{T}^s$ to the element $v\in\mathcal{U}^s$ defined by $v=Iu$. This would make $\mathcal{T}^{-\infty}$ a subspace of $\mathcal{U}^{-\infty}$ and we would have the continuous inclusions $\mathcal{T}^s\subset\mathcal{U}^s$ for all $s\in\mathbb{R}$, and $\mathcal{U}^s\subset\mathcal{T}^{s-1}$ for all $s>\frac{1}{2}$. However, there is a fatal flaw in this reasoning, which is that $I:\mathcal{T}^s\to\mathcal{U}^s$ is not injective for all $s\in\mathbb{R}$. A good way to see this is by looking at the element $u=\frac{1}{\omega}\in\mathcal{U}^0$, and letting

$$v:=(\omega\partial_{x_1}\omega)u.$$

By Lemma 2.9, $v\in\mathcal{T}^{-1}$, and by definition of $\omega\nabla\omega$, one has

$$\begin{aligned}\hat{v}_l^m &= 2\left((\omega\partial_{x_1}\omega)\frac{1}{\omega},T_l^m\right)_{\frac{1}{\omega}}\\ &= -2\left(\frac{1}{\omega},\partial_{x_1}T_l^m\right)_{\omega}\\ &= -2\int_{\mathbb{D}}\partial_{x_1}\overline{T_l^m(x)}\,\mathrm{d}x\\ &= -2\int_{\partial\mathbb{D}}\xi_1\overline{T_l^m(\xi)}\,\mathrm{d}\xi.\end{aligned}$$

One can check that $\hat{v}_l^m$ is not 0 for example for $l = m = 1$ (notice how v is "supported on $\partial\mathbb{D}$", in the sense that $(v, f)_{\frac{1}{\omega}} = 0$ whenever f vanishes on $\partial\mathbb{D}$). Now, let $w = Iv$. For all $(l, m) \in \Lambda$, we have by definition

$$\begin{aligned}\check{w}_l^m &= j_{l+1}^m \hat{v}_l^m + j_{l+2}^m \hat{v}_{l+2}^m \\ &= -2\int_{\partial\mathbb{D}} \xi_1 \left(j_{l+1}^m \overline{T_l^m} + j_{l+2}^m \overline{T}_{l+2}^m \right) \mathrm{d}\xi \\ &= -2\int_{\partial\mathbb{D}} \xi_1 \omega^2(\xi) \overline{U}_l^m(\xi)\, \mathrm{d}\xi \\ &= 0\end{aligned},$$

where we used the identity (A.4) and the fact that the weight ω vanishes on $\partial\mathbb{D}$. Hence $w = 0$ so I is not injective on $\mathcal{T}^{-1}$. In fact, one should not view I as an identity operator, but rather as a restriction operator from $\overline{\mathbb{D}}$ to $\mathbb{D}$. Its kernel contains elements of $\mathcal{T}^s$ supported in $\partial\mathbb{D}$. For $s \geq 0$, this kernel is simply $\{0\}$, but it can be larger for general s (just like for $s \leq -1/2$, the set of distributions of $H^s(\Omega)$ supported in $\partial\Omega$ is strictly larger than $\{0\}$).

Proof of Theorem 2.13. The inclusions shown above imply at once that $\mathcal{T}^\infty = \mathcal{U}^\infty$. By Lemma 2.5, $C^\infty(\overline{\mathbb{D}}) \subset \mathcal{T}^\infty$. To show the converse inclusion, we first remark that if $u \in \mathcal{T}^\infty$, then the decomposition of u on the functions T_l^m converges uniformly, as can be seen using the estimate (6). This implies that $\mathcal{T}^\infty \subset C^0$. Furthermore, by Lemma 2.9, if $u \in \mathcal{T}^\infty$, each component of ∇u is in $\mathcal{U}^\infty = \mathcal{T}^\infty$ and is therefore continuous. The proof is then concluded by a bootstrap argument. □

Data availability statement

The research code associated with this article is openly available in GitHub https://github.com/MartinAverseng/SqPrecondDiskScreen and Zenodo DOI: 10.5281/zenodo.7991556 [7].

References

[1] M. Abramowitz and I.A. Stegun, Handbook of Mathematical Functions With Formulas, Graphs, and Mathematical Tables. Vol. 55 of *National Bureau of Standards Applied Mathematics Series*. US Government Printing Office (1964).

[2] F. Alouges and M. Aussal, FEM and BEM simulations with the Gypsilab framework. *SMAI J. Comput. Math.* **4** (2018) 297–318.

[3] F. Alouges and M. Averseng, New preconditioners for the Laplace and Helmholtz integral equations on open curves: analytical framework and numerical results. *Numer. Math.* **148** (2021) 255–292.

[4] F. Alouges, S. Borel and D.P. Levadoux, A stable well-conditioned integral equation for electromagnetism scattering. *J. Comput. Appl. Math.* **204** (2007) 440–451.

[5] X. Antoine and M. Darbas, Generalized combined field integral equations for the iterative solution of the three-dimensional helmholtz equation. *ESAIM: Math. Modell. Numer. Anal.* **41** (2007) 147–167.

[6] M. Averseng, Pseudo-differential analysis of the Helmholtz layer potentials on open curves. Preprint arXiv:1905.13604 (2019).

[7] M. Averseng, Square-root preconditioners for the disk screen in Matlab. https://github.com/MartinAverseng/SqPrecondDiskScreen (2022). DOI: 10.5281/zenodo.7991556.

[8] M. Averseng, Stability of a weighted L^2 projection in weighted Sobolev spaces. *C. R. Math.* **361** (2023) 757–766.

[9] R.E. Bank and T. Dupont, An optimal order process for solving finite element equations. *Math. Comput.* **36** (1981) 35–51.

[10] O.P. Bruno and S.K. Lintner, Second-kind integral solvers for TE and TM problems of diffraction by open arcs. *Radio Sci.* **47** (2012) 1–13.

[11] S.H. Christiansen and J.-C. Nédélec, Des préconditionneurs pour la résolution numérique des équations intégrales de frontière de l'acoustique. *Comptes Rendus de l'Académie des Sciences-Series I-Mathematics* **330** (2000) 617–622.

[12] D. Colton and R. Kress, Integral Equation Methods in Scattering Theory. SIAM (2013).

[13] M. Costabel, M. Dauge and R. Duduchava, Asymptotics Without Logarithmic Terms for Crack Problems. Taylor & Francis (2003).

[14] C. Flammer, Spheroidal Wave Functions. Courier Corporation (2014).

[15] J. Galkowski, E.H. Muller and E.A. Spence, Wavenumber-explicit analysis for the Helmholtz h-BEM: error estimates and iteration counts for the Dirichlet problem. *Numer. Math.* **142** (2019) 329–357.

[16] M.J. Gander, I.G. Graham and E.A. Spence, Applying GMRES to the Helmholtz equation with shifted Laplacian preconditioning: What is the largest shift for which wavenumber-independent convergence is guaranteed? *Numer. Math.* **131** (2015) 567–614.

[17] Z. Gimbutas and L. Greengard, Computational software: simple fmm libraries for electrostatics, slow viscous flow, and frequency-domain wave propagation. *Commun. Comput. Phys.* **18** (2015) 516–528.
[18] H. Gimperlein, J. Stocek and C. Urzúa-Torres, Optimal operator preconditioning for pseudodifferential boundary problems. *Numer. Math.* **148** (2021) 1–41.
[19] I.G. Graham and W. McLean, Anisotropic mesh refinement: the conditioning of Galerkin boundary element matrices and simple preconditioners. *SIAM J. Numer. Anal.* **44** (2006) 1487–1513.
[20] L. Greengard and V. Rokhlin, A fast algorithm for particle simulations. *J. Comput. Phys.* **73** (1987) 325–348.
[21] W. Hackbusch, A sparse matrix arithmetic based on $\mathcal{H}$-matrices. Part I: introduction to $\mathcal{H}$-matrices. *Computing* **62** (1999) 89–108.
[22] N. Hale, N.J. Higham and L.N. Trefethen, Computing A^α, $\log(A)$, and related matrix functions by contour integrals. *SIAM J. Numer. Anal.* **46** (2008) 2505–2523.
[23] R. Hiptmair, Operator preconditioning. *Comput. Math. Appl.* **52** (2006) 699–706.
[24] R. Hiptmair, C. Jerez-Hanckes and C. Urzúa-Torres, Mesh-independent operator preconditioning for boundary elements on open curves. *SIAM J. Numer. Anal.* **52** (2014) 2295–2314.
[25] R. Hiptmair, C. Jerez-Hanckes and C. Urzúa-Torres, Closed-form inverses of the weakly singular and hypersingular operators on disks. *Integral Equ.Oper. Theory* **90** (2018) 1–14.
[26] R. Hiptmair, C. Jerez-Hanckes and C. Urzúa-Torres, Optimal operator preconditioning for Galerkin boundary element methods on 3-dimensional screens. *SIAM J. Numer. Anal.* **58** (2020) 834–857.
[27] H. Holm, M. Maischak and E.P. Stephan, The hp-version of the boundary element method for Helmholtz screen problems. *Computing* **57** (1996) 105–134.
[28] R. Hurri, The weighted Poincaré inequalities. *Math. Scand.* **67** (1990) 145–160.
[29] D. Kershaw, Some extensions of W. Gautschi's inequalities for the gamma function. *Math. Comp.* **41** (1983) 607–611.
[30] Y.Y. Lu, A Padé approximation method for square roots of symmetric positive definite matrices. *SIAM J. Matrix Anal. App.* **19** (1998) 833–845.
[31] W. McLean, Strongly Elliptic Systems and Boundary Integral Equations. Cambridge University Press, Cambridge (2000).
[32] F.A. Milinazzo, C.A. Zala and G.H. Brooke, Rational square-root approximations for parabolic equation algorithms. *J. Acoust. Soc. Amer.* **101** (1997) 760–766.
[33] N.M. Nachtigal, S.C. Reddy and L.N. Trefethen, How fast are nonsymmetric matrix iterations? *SIAM J. Matrix Anal. App.* **13** (1992) 778–795.
[34] J.-C. Nédélec, Acoustic and Electromagnetic Equations: Integral Representations for Harmonic Problems. Vol. 144 of *Applied Mathematical Sciences*. Springer-Verlag, New York (2001).
[35] C. Pechstein and R. Scheichl, Weighted Poincaré inequalities. *IMA J. Numer. Anal.* **33** (2013) 652–686.
[36] P. Ramaciotti, *Theoretical and numerical aspects of wave propagation phenomena in complex domains and applications to remote sensing*. Ph.D. thesis, Université Paris-Saclay (ComUE) (2016).
[37] P. Ramaciotti and J.-C. Nédélec, About some boundary integral operators on the unit disk related to the Laplace equation. *SIAM J. Numer. Anal.* **55** (2017) 1892–1914.
[38] V. Rokhlin, Diagonal forms of translation operators for the Helmholtz equation in three dimensions. *Appl. Comput. Harmonic Anal.* **1** (1993) 82–93.
[39] Y. Saad and M.H. Schultz, GMRES: a generalized minimal residual algorithm for solving nonsymmetric linear systems. *SIAM J. Sci. Stat. Comput.* **7** (1986) 856–869.
[40] S.A. Sauter and C. Schwab, Boundary Element Methods. Springer Series in Computational Mathematics. Springer-Verlag, Berlin (2011).
[41] O. Steinbach and W.L. Wendland, The construction of some efficient preconditioners in the boundary element method. *Adv. Comput. Math.* **9** (1998) 191–216.
[42] E.P. Stephan, Boundary integral equations for screen problems in $\mathbb{R}^3$. *Integral Equ. Oper. Theory* **10** (1987) 236–257.
[43] E.P. Stephan, The hp boundary element method for solving 2-and 3-dimensional problems. *Comput. Methods Appl. Mech. Eng.* **133** (1996) 183–208.
[44] A. Veeser, Approximating gradients with continuous piecewise polynomial functions. *Found. Comput. Math.* **16** (2016) 723–750.